



**HAL**  
open science

## Deep eutectic solvents (DESs): A short overview of the thermophysical properties and current use as base fluid for heat transfer nanofluids

Kimia Jafari, Mohammad Hossein Fatemi, Patrice Estellé

### ► To cite this version:

Kimia Jafari, Mohammad Hossein Fatemi, Patrice Estellé. Deep eutectic solvents (DESs): A short overview of the thermophysical properties and current use as base fluid for heat transfer nanofluids. *Journal of Molecular Liquids*, 2021, 321, pp.114752. 10.1016/j.molliq.2020.114752 . hal-03127453

**HAL Id: hal-03127453**

**<https://hal.science/hal-03127453v1>**

Submitted on 18 Feb 2021

**HAL** is a multi-disciplinary open access archive for the deposit and dissemination of scientific research documents, whether they are published or not. The documents may come from teaching and research institutions in France or abroad, or from public or private research centers.

L'archive ouverte pluridisciplinaire **HAL**, est destinée au dépôt et à la diffusion de documents scientifiques de niveau recherche, publiés ou non, émanant des établissements d'enseignement et de recherche français ou étrangers, des laboratoires publics ou privés.

# Deep eutectic solvents (DESs): a short overview of the thermophysical properties and current use as base fluid for heat transfer nanofluids

Kimia Jafari<sup>a</sup>, Mohammad Hossein Fatemi<sup>a</sup>, Patrice Estelle<sup>b,\*</sup>

<sup>a</sup> Chemometrics Laboratory, Faculty of Chemistry, University of Mazandaran, Babolsar, Iran

<sup>b</sup> Univ Rennes, LGCGM, F-35000 Rennes, France

\* **Corresponding Author**, Email: patrice.estelle@univ-rennes1.fr ORCID: orcid.org/0000-0003-3305-7831

## Abstract

Nowadays, different types of strategies are proposed and tested to find the best scenario for upgrading the productivity of heat transfer fluids, especially nanofluids. Some optimum empirical conditions demonstrated that the best size, shape, and nature of nanoparticles and their appropriate dispersion have positive influences on nanofluid thermal conductivity improvements. Therefore, the specific physicochemical properties of the base fluid can be taken into account as one of the decisive factors in heat transfer operations. Deep eutectic solvents (DESs) are nominated as valuable materials to meet the demands for sustainable ecological processes and open opportunities for overcoming the limitations of conventional fluids.

The purpose of this study is to briefly introduce the DESs for evaluating their thermal potential applicability and their use to produce nanofluids. DES-based nanofluids represent a new and creative type of heat transfer fluids that possess high potential in different target applications and are not harmful to the environment. This type of nanofluid has higher thermal properties than the base DESs. Increasing the temperature and the volume fraction of nanoparticles lead to further increment in their thermal properties. In this study, the chemical structure and preparation method have been addressed for the DES and DES-based nanofluids. Also, the theoretical approaches have been considered for modeling and predicting their behavior. A discussion was extended to investigate the usage of DES as host fluid for producing nanofluids, and its advantages and drawbacks are also presented. It is deduced that the DES-based nanofluids are one of the smart choices for the progression of nanofluids and give the most promising results for application in heat transport fluids. The contents may shed light on a detailed awareness of the heat transfer potential of the DESs.

Nomenclature		Hydrogen bond donor	TGA	
AARD	Average absolute relative deviation	H-NMR		Thermal gravimetric analysis
ANN	Artificial neural network	IA	UV	Ultra violet spectroscopy
bf	Base fluid	IEP	VG	Geometric variance
BTPC	Benzyltriphenyl phosphonium chloride	IL	XPS	X-ray photoelectron spectroscopy
ChCl	Choline chloride	MD		
C-MAS-NMR	<sup>13</sup> C-magic angle spinning-NMR	MEA	XRD	X-ray powder diffraction
C-NMR	Carbon nuclear magnetic resonance	MG		
CNT	Carbon nanotube	MIP		
cP	Centi poise (1P = 1 g.cm <sup>-1</sup> .s <sup>-1</sup> )	MPTMS		
CSP	Concentrated solar power			
DAC	N,N diethylethanolammium chloride	MTPB		
DBSA-PANI	Dodecyl benzene sulfonic acid doped polyaniline			
DEA	Diethanolamine	MWCNT		
DES	Deep eutectic solvent			
DNA	Deoxyribonucleic acid	N		
DP	2-butoxy-3,4-dihydropyran	NADES		
DSC	Differential scanning calorimetry	Nf		
EG	Ethylene glycol	NMSE		
FB	Fractional bias			
FT-IR	Fourier-transform infrared spectroscopy	R <sup>2</sup>		
HBA	Hydrogen bond acceptor	Re		
HBD		rpm		
		SEM		
		TBAB		
		TEG		
		TEM		
		TEOS		

The performance or compactness of engineering apparatus (e.g., electronic devices and heat exchangers) faces with the consequential limitation arising from low thermal conductivity of classical heat transfer fluids (e.g., water, ethylene glycol, and their binary mixture). Due to the economic issues, the heat transport optimization in such energy systems and technical devices is an appreciable motivation to propose the existing fluids with higher heat transport potential [1,2]. Choi and Eastman [3], proposed an innovative approach by incorporating particles of nano-sized in classic liquids. The results revealed that it can beneficially lead to the improvement of thermal conductivity. The nanofluids can improve thermal properties higher than the ordinary liquids. In general, nanofluids are one of the unique generations of the thermal fluids prepared by the dispersion of particles with the size range of 1-100 nm (e.g., metallic, polymeric, and carbon-based nanoparticles) in a conventional working liquid (e.g., water, transfer oil, ethylene glycol, glycerol, and so forth). The preparation is performed by either one-step or two-step methods as explained in previous works [4–6]. To investigate the fundamental mechanism and evolve the potential of nanofluids, further analysis was conducted for improving their properties [7–10].

One of the main limitations of organic solvents is toxicity and elevated cost owing to their manufacture and purification process. In other words, there is a public confront about the concept of safety of materials both in production and application, which requires serious attention. In addition to economic concerns, the urgency of adaptation to nature is the uppermost argument to move towards green solvents. Nowadays, nature invites us to make more environment-oriented and sustainable decisions for the progression of industries. Despite the minor defects of green solvents, it is essential to spend more time and energy to use green solvents as heat transfer fluid. It is necessary to find a solution that not only remedies the undeniable negative impacts of toxic materials in the advance of scientific purposes and industries (it is done by focusing on the outline of green-based alternatives within industrial chemical processes) but also provides the benefits of the previous two scenarios [11–13]. The ionic liquids (ILs) are the first alternative that is offered instead of the conventional base fluids.

The ILs are taken into account as an interesting solvent formed of the large inorganic/organic anions and organic cations that persist in liquid state at/near ambient temperature and could participate in a various range of interactions such as van der Waals, coulombic, hydrogen bonding, dipole-dipole, and magnetic dipole interactions in magnetic ionic liquids as specific [14,15]. In each combination (anions and cations), a variation in objective fabricates a fresh solvent, and thus the ILs become designable to achieve desired industrial and/or scientific goals. Besides, these combinations not only have negligible vapor pressure, less volatility, and a wide liquid temperature range, but also contain non-flammable substances and ready for dissolving inorganic and organic compounds [16,17]. Meanwhile, these blends are surrounded by expensive

become an interesting topic to the nanofluid community. Hosseinghorbani et al. [19] dispersed three different mass fractions of 0.5%, 1% and 2% for graphene oxide nanoparticles in 1-butyl-3-methylimidazolium bis(trifluoromethylsulfonyl)imide ([Bmim][NTf<sub>2</sub>]) to fabricate stable nanofluids. The prepared nanofluids had fine stability for up to two weeks without any surfactant application. Then, thermophysical properties were measured for the IL and nanofluids based on IL. The results of the comparison between experimental data indicated that specific heat capacity and thermal conductivity increase up to 42% and, 6.5% at 2% mass fraction, respectively. Bridges et al. [20] studied heat capacity, the density of [C<sub>4</sub>mim][NTf<sub>2</sub>], and IL-based nanofluids with 50 and 4 nm alumina and carbon black (CB), respectively. They observed that density has increased by about 10% for Al<sub>2</sub>O<sub>3</sub>-based nanofluids, but it has decreased by 10% for CB-based nanofluids. Also, it was reported that heat capacity has increased 40% for the Al<sub>2</sub>O<sub>3</sub>-based nanofluids and it has decreased 30% for the CB-based nanofluids. Visser et al. [21] investigated the effect of alumina nanoparticles on the physicochemical properties of several ILs, including 1-butyl-3-methylimidazolium bis(trifluoromethylsulfonyl)imide ([C<sub>4</sub>mim][Tf<sub>2</sub>N]), 1-butyl-2,3-dimethylimidazolium bis(trifluoromethylsulfonyl)imide ([C<sub>4</sub>mmim][Tf<sub>2</sub>N]), and 1-butyl-3-methylimidazolium bis(perfluoroethylsulfonyl)imide ([C<sub>4</sub>mim][BETI]), respectively. Meanwhile some ionanofluids were prepared in [Bmim][PF<sub>6</sub>], [C<sub>4</sub>mim][Br], and [C<sub>4</sub>mim]PF<sub>6</sub>, for example Wang et al. [22] and Shevelyova et al. [23], which due to their corrosion problems (caused by their reactivity with water leads to production of corrosive hydrogen fluoride acid) had not remarkable superiority. So, preparation of nanofluids based on any ionic liquid containing [PF<sub>6</sub>]<sup>-</sup> and [BF<sub>4</sub>]<sup>-</sup> anions are not recommend [24,25]. The aforementioned reports were several remarkable studies on the use of ILs as a base liquid to produce nanofluid. More details on this topic can be found in the literature [26–28]. Although these compounds had remarkable superiority, it was not enough to achieve a sustainable heat transfer solvent. The ILs were not often satisfying as enough. It was due to the restrictions such as high-price, hard-synthesize, and highly viscous. Before emerging deep eutectic solvents (DESs), various attempts have been performed to find a potentially less harmful fluid to nature.

A logical mixture of two (or more) components (i.e., organic halide salts and hydrogen bond donors (HBD)) is incorporated by the hydrogen bond interactions, resulting in establishing a homogeneous solvent, namely deep eutectic solvent [29–31]. The created solvent has a melting point lower than 373 K and either component. There is a wide range of possible variables to be engaged in the DES structural network such as HBD and HBA. These have mostly interacted with hydrogen bonds besides van der Waals forces. The most common HBAs are quaternary phosphonium or ammonium salts. Among them, choline chloride is the most popular HBA for preparing the DESs. The HBAs are combined with HBDs to form the DESs. In this case, various substances are used as HBDs, including diols, alcohols, phenol derivatives, carboxylic acids,

am ent

components, the DESs can be designed purposefully similar to the ILs. In this regard, the DESs are initially recognized. This step is similar to the new generation of the ILs. However, their aspects are approved after a short time. Thus, the DESs can properly be defined as a distinguished type of solvents [33]. There were strong reasons for detaching these two types of solvents: (I) the synthesis process of the DES is quite simple, time-saving, and no purification required, whereas, preparing the ILs is expensive and more complicated than the DES; (II) the principal interactions between ingredients are mainly hydrogen and ionic bonds in the DES and ILs, respectively; (III) the DES is safer and cheaper than the ILs, so it is better adapted to usage on the upper scale [17,30,33–39]. Nowadays, these are known as a better version of the ILs. The most eminent merits of the DESs can be represented as follow: (i) simplicity of preparation, (ii) high heat capacity, (iii) high moisture stability, (iv) low melting point, (v) low volatility, (vi) low density, (vii) insignificant vapor pressure, (viii) water-compatible, (ix) non-flammability, and (x) biologically compatible [31,40]. What should be considered about solvents, which used as base fluids, is that their suitable volatility. If a liquid has higher vaporizing tendency, will produce vapors more easily than liquid with lower vapor pressure at same temperature. For usage of volatile compounds in heat transfer systems, the system has to be either engineered to prevent the phase change (i.e. volatilization and condensation) through pressurization of the system or operated across the phase change. The insignificant vapor pressure of DESs would lead to a simplification of the design if used as a thermal fluid. Additionally, these are both inexpensive and their broad range of variety shows that it's quite profitable. Fig. 1 characterizes the eminent benefits of the DES. Although their high viscosity and solid state at room temperature could be negative, compatibility with water and the possibility to design ternary blends might be helpful [41–43]. Although the DES is a fairly well-developed subject area in chemistry, it is only the beginning of finding favor with engineers [44]. This is especially true for industrial scientists. Some reasons for happening this issue are comprised of the constantly increasing demand for industrial development by eco-friendly materials and emphasizing the fabrication and utilization of multi-task approaches. The DESs are considered as one of the worthy alternatives to common thermal fluid in comparison with previous fluids such as organic solvents or ILs. Although the usage of DESs in heat transfer operations is still at the beginning stages, these are increasingly applied in the various fields of chemistry. Fig. 2 illustrates some well-known applications for the DES. Water was taken into account as the common electrolyte used in electrodeposited coatings operations, which had some restrictions in nature (e.g., a limited potential window and high hydrogen evolution under certain industrial circumstances). These shortcomings are currently covered by using the DES for metal plating. Therefore, the final mechanical qualities of the deposits and sensor technology are improved [45–48]. Over the last years, it has been reported that the DES is a suitable medium for the provision of polymeric materials with advanced morphological and functional specifications. The DESs are

use of carbon electrodes for capacitors [49], utilizing as an efficient solvent for the selective extraction and separation of different bioactive substances (e.g., phytocannabinoids, flavonoids, etc.) [50–52], as well as using as adsorbents for removing heavy metals (e.g., lead, mercury, and arsenic from water) [53], and usage in dye-sensitized solar cells as an electrolyte [54]. There are many valuable reviews on different aspects of progress these solvents [30,35,55,56].

This study is focused on describing the preparation method and various types of DESs. Besides, some of the reported empirical findings are examined. Several opportunities are also identified for future research by explaining the DES applications. Furthermore, studies that have used the DES as a base fluid including nanoparticles are analyzed in detail, and thus valuable information is given to readers about the DES-based nanofluids. Indeed, the contribution of this study is to answer the question: what are the DESs and their potential character in heat transfer?

## 2. Preparation of DES

As mentioned before, the DES is formed by (at least) two main components, consisting of a donor and an acceptor to the foundation of stable hydrogen bonds. The quaternary ammonium salts and phosphate salts are regularly used as the HBA. Whereas, there is a wide range of choices for the HBD, entailing alcohols, organic acids, and amines in which everyone renders a specific characteristic to the related DES. The choline chloride (ChCl) is used as the most widespread HBA considering its properties [31,57]. The ChCl is an inexpensive and biocompatible quaternary ammonium salt that is successfully applied to produce the DES using HBAs such as urea, polyols, imidazole derivatives, and carboxylic acids [31,40,58,59]. Table 1 gives some ordinary HBAs and HBDs together with their chemical structure.

Recently, natural deep eutectic solvents (NADESs) were recognized as the main sub-class of the DES. The solubility of biomolecules (e.g., albumin, starch, and DNA) in NADESs is higher than water. Also, they have the potential to be employed as an extraction media for bioactive combinations [60,61]. The HBDs and HBAs are chosen for constructing the NADESs via the following categories: organic acids, alcohols, sugars, ChCl, and amino acids [62]. The diversity of raw constitutes makes it possible to form a broad array for different blends so that more than a hundred NADESs have been reported to date [56]. Due to the natural origination, it could be stated that the NADESs are more eco-label than other DESs.

Generally, the process of preparation is entirely simple and purification-free together with a 100% atom efficiency. This process is performed by mixing HBD and HBA at a convenient temperature. In this process, the component with a lower melting point is firstly melted and subsequently, the other component is added to be melted with each other, and then it is stirred until reaching a homogeneous liquid [63]. In this case, the

DES with a high potential thermal character. The certain molar ratio of HBA and HBD should make the possible mixture to touch the eutectic point [29–31]. Open to question is whether the tested molar ratio induces strong association and formation of homogeneous solvent. If the available resources do not represent a suitable proportion for each combination of reactants to produce stable DES (some worthy examples are provided in Table 2), the optimum molar ratio can be found by conducting a primary screening [33,64–81]. For example, Ibrahim et al. [82] used EG to test 51 different ratios of the ammonium and phosphonium salts, and thus the homogeneous DES is synthesized using a magnetic stirrer at atmospheric pressure and under controllable empirical conditions. Every combination of salt and HBD was mixed at 180 rpm for a period of 80 minutes at a temperature of 343.15 K. It was observed that some examined ratios were failed to produce a uniform solvent. As a result, some precipitates appeared or the solvent turned into solid/semisolid form. Finally, five specific ratios were achieved considering the related stability of the solvent, including 1:3 methyl-triphenylphosphonium-bromide (MTPB):EG, 1:2 ChCl:EG, 1:3 N,N diethylethanolammium chloride (DAC):EG, 1:11 benzyltriphenylphosphoniumchloride (BTPC):EG, and 1:2 tetra-n-butylammonium bromide (TBAB):EG. It should be noted that all composed DESs were saved in controlled ambient moisture. The so-called reline mixture was obtained by a 1:2 molar ratio of ChCl and urea at room temperature. It was recognized as the first report of the DES represented by Abbott et al. [63]. Hou et al. [83] reported a 3:7 molar ratio for imidazole and ChCl. Abbott et al. [32] formed some DES by 1:1 molar ratio of adipic acid, benzoic acid, citric acid, and oxalic acid as the HBD and ChCl as the HBA. Carriazo et al. [84] presented a stable solvent by 1:4 of resorcinol:ChCl. Abbott et al. [63] also prepared several steady-state DESs with different constituents by 1:2 molar ratio involving thiourea:ChCl, acetamide:ChCl, 1,3-dimethyl urea:ChCl, 1-methyl urea:ChCl, 1,1-dimethyl urea:ChCl, and benzamide:ChCl.

To find the right molar ratio of DES for using as thermal conductive fluid, different proportions are composed, and then thermal conductivity and viscosity are measured for all of them. The best combination coincides with the highest thermal conductivity and lowest viscosity. As an example, Liu et al. [85] first prepared four distinct proportions of glycerol and ChCl as 2:1, 3:1, 4:1, and 5:1 for producing DES, respectively. Thus, a high potential graphene oxide-based nanofluid was traced. By evaluating the thermal conductivity, viscosity, boiling, and freezing points, a molar ratio of 3:1 was selected as the optimum DES. Therefore, the preferred quality is assigned to the solvent by picking out its components.

There are different techniques for confirming the synthesis of DES, such as FT-IR spectroscopy. The FT-IR spectroscopy investigates the structure of DES by identifying the functional groups and revealing the interactions between the atoms of components [86]. There are also some other analyses for inspecting the



widely used techniques are comprised of the TGA (it is used for measuring thermal stability),  $^1\text{H-NMR}$  (it is correlated to the number of hydrogens and their positions in the chemical structure of DES), differential scanning calorimetry (DSC) (it highlights the formation of DES), and  $^{13}\text{C-NMR}$  [86–88].

## 2-1. Preparation DES-based nanofluids

In the previous section, it was mentioned that the optimal selection of HBD and HBA is a great deal to construct the DES quality (quality is referred to as the preferable thermal properties). Preparing nanofluids based on the DES is a major challenging problem, which is due to the fact that the nanoparticles must not chemically react to the base fluid. The preparation of DES-based nanofluids is not easier in comparison with water-based ones, but nanofluids based on DESs have more simple produce process than IL-based nanofluids. The two-step method is often used for the preparation process. Hence, the DES-based nanofluids are constituted by the dispersal of dried powder of nanoparticles into the DES. Another important issue is concerned with the tendency of nanoparticles towards the agglomeration. This is due to the presence of van der Waals attraction force, which arises from their surface activity and huge surface area. The aggregation of particles has a negative effect on the thermal properties enhancement [89]. Therefore, it is essential to have a stable nanofluid during the analysis procedure and usage of nanofluids. The agglomeration issue can be resolved by employing specific solutions, and thus a stable nanofluid is created. These solutions are categorized into two main classes, including dispersion techniques and stabilization techniques. The dispersion techniques are applied to break agglomerates formed during the nanoparticle production. The stabilization techniques can avoid re-agglomeration of nanoparticles when they break down close to their primary particle size. It is performed because of van der Waals forces and using electrostatic, steric, or electrosteric repulsive forces. One of the dispersion techniques is sonication, and the most common stabilization methods are comprised of surfactants, pH control, and surface modifications, which are described as follows: (1) Surfactants: the addition of surfactants is one of the most popular approaches to prevent sedimentation. This is also a low-cost and effortless technique. On the other hand, most of the methods cannot tolerate temperatures of higher than 333 K, and their presence can lead to the augmentation of the thermal resistance and limitation of the thermal conductivity enhancement [90]. (2) pH controlling: the electrokinetic features have a consistent influence on stability, which could be controlled by regulating pH. In this regard, the isoelectric point is initially defined (the pH value is zero at the overall electric charge of the molecule) [91]. Then, the pH value is modified to augment potent repulsive forces. It is carried out by the preparation of a uniform stable nanofluid [4]. Different nanofluid possesses various pH values of IEP and the fluctuation of temperature changes the pH value of IP [92]. These circumstances become more complex when the nature of HBD and HBA are also considered. Thereby, it is a strong scenario, but its

res] ace  
of nanoparticles changes by a directed chemical reaction. It is due to the characteristics and nature of the particles and base fluid. Despite the control of the reaction process is tough, it requires the highest precision as a matter of course [93]. Since the DESs are also a desirable environment for synthesis purposes, this is a key strategy that can seriously be considered for the implementation procedure. (4) Sonication: ultrasonic vibration is considered as the most frequent effective method for sustaining the well-dispersed suspensions and producing the long-time stable nanofluids. This technique collapses the assemblage of nanoparticles into the smaller aggregates without any change in their surface properties. Meanwhile, even individual nanoparticles simply perform in the same manner. It appears that both ultrasonication time and its power are effective on dispersion and thermal conductivity enhancement. Also, the ultrasonic probe devices have better performance than ultrasonic bath devices [94,95]. Among the mentioned techniques, ultrasonic treatment is an optimal technique from operation cost and time point of view. This technique prepares a homogenous dispersion, especially in the case of the DES-based nanofluids.

As an example, Liu et al. [85] prepared a stable nanofluid of graphene oxide-DES by implementing the following steps. First, the appropriate molar ratios of glycerol and ChCl were mixed at 373 K and stirred for one hour. The uniform solvent was created after cooling and reaching ambient temperature. Second, 12.6 g of glycerol:ChCl with 80 mg graphene oxide in a 50 mL sealed glass tube was mixed by a magnetic stirrer at 373 K for two hours. Afterward, it was cooled at room temperature for 2 hours, and sonication was applied to attain a stable nanofluid.

As another example, Liu et al. [90] developed a typical preparation procedure to form a DES-based nanofluid by a combination of silica nanoparticle and glycerol:ChCl. According to this method, 100 ml of DES was mixed with a certain mass fraction of silica nanoparticle, and then the resulting combination was stirred for 2 hours at 353 K, subsequently, it was cooled to reach room temperature. Finally, the suspension was subjected to sonication for 2 hours to reach uniformity, and thus the stability was amplified for the final nanofluid.

### 3. Characterization of DES

The assessment of thermophysical properties (e.g., thermal conductivity, viscosity, and density) can efficiently be used for finding a worthy option. The experimental data collection and the specifications of DESs can be investigated in future research. Over the past years, numerous papers have been published by focusing on the development and characterization of DES properties. The results of these papers showed that the DESs can be considered as desirable potential options for heat transfer purposes. Table 3 provides a summary of some studies on the thermophysical properties of the DESs.

Generally, the thermal conductivity is the most important parameter for improving heat transfer performance. The transient hot wire is widely used for measuring the thermal conductivity of DES and nanofluids (e.g., temperature oscillation and steady-state parallel plate) [97,98]. Although the conventional properties of DESs have widely been investigated, there is a significant gap between specific studies on thermal conductivity. Fig. 3 depicts the changes in thermal conductivity against temperature for three different DESs, (reported by Gautam et al. [99]). Nevertheless, it is essential to develop a comprehensive study, consisting of further experimental examinations and deeper analyses under control conditions. Thus, the exact effect of various parameters is determined such as water content and type of HBD/HBA. This issue could help us to perceive the nature of solvent systems and expedite their potential applications in different fields.

### 3-2. Viscosity

Since the viscosity can determine the required pumping power of fluids [100], it is a very important factor among the thermophysical properties. So, it is necessary to investigate the variations in viscosity. Fig. 4 represents the previous viscosity data for different DESs as a function of temperature. One of the foremost drawbacks of the DES is dealt with the high viscosity of some of them. This is a very important issue, especially when a solvent is designed for industrial purposes [101]. Several plans were offered to decline viscosity, and thus the application of these promising green solvents has enhanced in the chemical industry. A combination of DES and water is an appropriate approach, which makes a soft structure between the ingredients of hydrogen bond [102,103]. Water is used not only to control viscosity of DES but also to improve thermophysical efficiency as a wisely decision, which is lead to water conservation in scientific and industrial purposes and at the same time take its thermophysical advantages. Lapena et al. [104] confirmed that water inclusion in  $\text{ChCl}:\text{EG}$  components has been led to a 30% decline in viscosity at 280 K. This slump is related to the interaction between water molecules and EG. This issue is remarkable, especially when the defined scheme of solvents requires their placements in channels and minimized-scale equipment.

In the majority of instances, the viscosity of DES is higher than 100 cP at ambient temperature [104–111]. This issue arises from the existence of an immense structural network of hydrogen bonds. Also, if big ions are selected as basic materials, their large size besides van der Waals or electrostatic interactions can amplify viscosity. Thus, the best offer is associated with selecting small cations or fluorinated HBDs to produce a DES with a low viscosity [112]. According to the Arrhenius behavior, it is observed that an increase in temperature leads to the reduction of viscosity.

### 3-3. Density

demonstrated that the vast majority of DESs possess higher density and the molar ratio of DES components has a significant effect on their density [33]. The difference between densities could be related to the different molecular arrangements in DES. Fig. 5 shows the density of some intended DES as a function of the temperature. As shown in Fig. 5, it is concluded that the linear reduction of density by increasing temperature is a general trend for DES. The behavior of density is interpreted by the hole theory because of its dependence on the molecular structure of DES. Mixing the HBA and HBD leads to a decrease in the average hole radius. Then, more free spaces become available, leading to density increment [33]. In general, the enhancement of temperature leads to a decrease in the alterations of DES density, and the value of density can be modified by selecting the type and proportion of HBA and HBD.

#### 4. Experimental studies on using DES as base fluid

In the following paragraphs, the influence of DES as a thermal fluid is investigated on the thermophysical properties of various nanofluids, and the most important findings are presented. Moreover, a summary of the relevant published studies is given in Table 4.

Fang et al. [113] have studied the thermophysical properties for graphene oxide nanoparticles in ammonium and phosphonium-based DES nanofluid. They prepared the samples through the two-step method in three different solid concentrations ranging from 0.01 to 0.05 wt% without surfactant. To investigate the stability of engineered nanofluids, visual observation (nanofluids were maintained for four weeks at room temperature), zeta potential (quantitative analysis of dispersed graphene oxide in 1:4 molar ratio of MTPB:EG), centrifuge technique (2 ml volume of nanofluids at four different rpms for 30 minutes at 298 K), and optical microscopy ( $\times 4$  magnification) were used to evaluate the uniformity of suspensions. Their observations showed that the stability enhances by increasing the presence of hydroxyl groups (increase in the amount of HBL) and decreasing the graphene oxide concentration. The outcomes of thermal conductivity measurements indicated that an increase in temperature from 298 K to 343 K leads to 85% and 177% thermal enhancements for nanofluids based on ChCl:triethylene glycol (TEG) (1:3) and MTPB:TEG (1:5), respectively. Moreover, it was found that the specific heat increases either by graphene oxide concentration or temperature.

Chen et al. [114] synthesized 33 various DESs using TEG and EG as HBDs, and ChCl and MTPB as halide salts in different molar ratios. By employing sonication, carbon nanotubes (CNTs) with concentrations 0.01–0.08 wt% were suspended into DESs, and thus stable nanofluids were prepared. Both visual observation and UV spectroscopy were employed to more accurately determine the stability of nanofluids. The inspections were revealed that the prepared nanofluids with DES composed by EG and

salt was stable just for one day. The stability data of nanofluids were 3 and 4 days in DESs synthesized from TEG with ammonium and phosphonium salts, respectively. Furthermore, they investigated the most common thermophysical properties. According to the general trend, it was observed that both the high temperature and concentration of CNT had a positive effect on thermal conductivity. Nanofluids based on EG showed 24.4% and 0.1% thermal enhancements. In this case, the maximum value was related to 0.08 wt%, 323 K, and 1:5 with ChCl. Also, the minimum value was related to 0.01 wt%, 298 K, and 1:3 with ChCl. Whereas, nanofluids based on TEG did not indicate any significant thermal improvement. The study of heat capacity changes demonstrated that the temperature and CNT concentration had positive and negative effects on the values of nanofluid specific heat, respectively. A reverse trend was observed for the viscosity and density of CNT-DES nanofluids.

Dehury et al. [100] synthesized a DES using oleic acid (as HBD) and DL-menthol (as HBA). They dispersed spherical nanoparticles of alumina in DES and measured its thermophysical properties. Thus, its potential was evaluated to be employed as a new thermal solvent. The thermal conductivity, heat capacity, density, and viscosity of DES and DES-based nanofluids were ascertained experimentally. A KD2 Pro thermal property analyzer was utilized to measure the thermal conductivity of DES (DL-menthol+oleic acid) and DES-based nanofluids (0.001, 0.005, 0.0075, and 0.01 volume fractions of alumina) in the range of 298.15-373.15 K. It was observed that the thermal enhancement of nanofluids was about 10% in comparison with the DES. The Bruggeman equation [115] was utilized to calculate the values of thermal conductivity. This equation is represented as follows:

$$k_{nf} = \frac{1}{4} [(3\varphi-1)k_n + (2+3\varphi)k_{DES}] + \frac{k_{DES}}{4} \sqrt{\Delta}$$

$$\Delta = \left[ (3\varphi-1)^2 \left( \frac{k_n}{k_{DES}} \right)^2 + (2-3\varphi)^2 + 2(2+9\varphi-9\varphi^2) \left( \frac{k_{DES}}{k_n} \right) \right] \quad (1)$$

where  $\varphi$  is the volume fraction of alumina,  $k_{DES}$ ,  $k_n$ , and  $k_{nf}$  are thermal conductivity of DES, nanoparticle, and nanofluid, respectively. Also, an increase in temperature has been led to the reduction of density, and their Newtonian behavior was confirmed by investigating viscosity [116]. The heat capacity of nanofluid was measured using a DSC and compared to the DES. The results demonstrated that heat capacities have enhanced by 6%, and 50% in 0.001, and 0.01 volume fractions, respectively. As an output, 0.005 volume fraction of alumina was reported as the optimum value. The thermal properties become more efficient by this optimum value.

Liu et al. [96] fabricated DES-based nanofluids by adding three different chemically modified silica nanoparticles (SiO<sub>2</sub>-SH, SiO<sub>2</sub>-SH-DP, and SiO<sub>2</sub>-SH-DP-Cu) to glycerol:ChCl and EG:ChCl solvents. Thus,

the samples were produced as follows: SiO<sub>2</sub>-SH fabricated by a sol-gel method from tetraethyl orthosilicate (TEOS) and (3-mercaptopropyl)trimethoxysilane (MPTMS), SiO<sub>2</sub>-SH-DP prepared by treatment of SiO<sub>2</sub>-SH with 2-butoxy-3,4-dihydropyran (DP) and facilitation of Lewis acid catalysis, and SiO<sub>2</sub>-SH-DP-Cu prepared by treatment of SiO<sub>2</sub>-SH-DP with Cu(acac)<sub>2</sub> and reduction of NaBH<sub>4</sub>. The chemical nature of the synthesized silica nanoparticles was carefully investigated via a complete and coherent survey. Thus, any changes were observed by the modification reactions. The SEM and TEM images, XRD spectra, FT-IR spectra, <sup>13</sup>C-MAS-NMR, TGA, and XPS analysis were carried out in a step by step procedure. The results demonstrated that the morphology of the revised silica is a monotonic sphere with an average size of 300 nm, the basic component of all nanoparticles remains SiO<sub>2</sub>, and the covalent bond effectually forms between silica and target modifier. After determining the stability of nanofluids, their performances were analyzed for 15 days at room temperature. This process was performed by measuring the thermal conductivity and viscosity. The thermal enhancements of 12.5% and 13.6% were achieved for glycerol:ChCl and EG:ChCl based nanofluids, respectively. The viscosity makes a unique behavior in the rich intermolecular hydrogen bonding included within the solvent. It was observed that the viscosity decreases until it reaches a mass fraction of 2.0%, and then it increases for higher content. Due to the fairly low concentration of hydrogen bonding, the effect of hydrogen bonding on EG:ChCl was weaker than glycerol:ChCl. The mechanism of stability enhancement was specified by molecular dynamic simulation.

The concentrated solar power (CSP) is taken into account as one of the worthwhile sources of renewable energy. In this regard, the up-gradation of the heat transfer coefficient of fluid should primarily be expanded to improve the efficiency of the solar plants. To find better choices for capacity storage, Dehury et al. [117] introduced a new thermal solvent, which is made of triphenylphosphonium bromide and EG. They produced a novel nanofluid by suspending a limited quantity of alumina nanoparticles with a size of 50 nm in the synthesized DES. The thermal conductivity has increased by 70% for this DES and its nanofluid in comparison with the commercial sample. Furthermore, it was observed that viscosity and density have decreased against temperature in agreement with the literature. The crosscheck of the thermophysical properties with the commercial cases (VP-1 and Dowtherm-A) confirmed that the introduced DES and its nanofluid give promising results for application as a low-cost thermal solvent at moderate temperatures.

Osama et al. [118] formed DES by EG and MTPB in 3:1 and 5:1 molar ratios. Then, they prepared nanofluids based on graphene oxide nanoparticles and studied their thermal behavior. They measured thermal conductivity in the temperature range of 298-343 K. It was observed that an increase in temperature has been led to the enhancement of the value of thermal conductivity in both DES-based nanofluids. However, there was no specific pattern for thermal conductivity enhancement versus the increment of

Brownian motion, Rashmi's [119] and Kumar's models [120]. These models will be described later. Thereafter, a new model was developed to predict the thermal conductivity of DES-based nanofluids. This model has higher accuracy than the aforementioned, called Kumar's modified model.

To investigate the possibility of using DES as a heat transfer fluid, Siong et al. [121] synthesized spherical nanoparticles, namely dodecyl benzene sulfonic acid doped polyaniline (DBSA-PANI). Then, they prepared DES-based nanofluids by a two-step method. The required DESs were simply made by implementing the following steps. First, ChCl and urea were mixed in 1:2 proportion and heated at 363 K (pure DES). Then, deionized water was added to the cooled mixture at room temperature and stirred for 15 minutes (DES with water). If the temperature has increased, the nanofluids based on DES with water showed higher improvement in thermal conductivity than the pure DES-based approach. The observed enhancement in the thermal conductivity of nanofluids was related to the Brownian motion of nanoparticles and micro-convection of base fluids along with the interaction between dopants and DES ions [22,122].

High thermal properties of DES, in particular at higher temperatures, encouraged Abdullah et al. [123] to examine the DES potential applicability as a host fluid in heat transfer purposes. The alumina-based nanofluids were generated by two different DESs, including ChCl:urea and ChCl:glycerol. Then, the modified Einstein's formula was used to assess their viscosity as a function of temperature (ranging from 303 to 343 K). It is observed that an increase in temperature has been led to the reduction of viscosity. This is associated with the expected trend. Although both DESs showed akin curves, ChCl:urea DES had a higher viscosity than ChCl:glycerol. It is due to the possibility of institution self-hydrogen bonds between the urea and chloride ions. To address the effect of alumina nanoparticles loading on the fluid friction factor, the following equation was used considering the studied conditions. Thus, the friction factor is computed for pure DES and nanofluids, which is valid for the laminar flow regime.

$$f = \frac{64}{Re} \quad (2)$$

$$Re = \frac{VD}{\vartheta}, \quad \vartheta = \frac{\mu}{\rho}$$

where  $V$  is the velocity of the fluid,  $D$  is the diameter of the tube,  $\vartheta$  is kinematic viscosity,  $\rho$  and  $\mu$  are density and viscosity, respectively. The results demonstrated that the existence of urea leads to the enhancement of viscosity. Consequently, it is found that the ChCl:urea has a higher friction factor than the other one. The previous studies [124,125] reported that a decrease in the  $Re$  number (it is caused by the increased nanoparticle) leads to the enhancement of friction factor. However, the friction factor of the studied DES was not affected by the increment of loading of nanoparticles. Furthermore, the effect of

the thermal conductivity was reported for the DESs. Overall, they found that the pure DESs have a higher heat transfer coefficient than their nanofluids. It happens due to the higher heat capacities for the DESs. Due to the unique properties of the DES, it was suggested to be employed at high temperatures.

In an interesting study, Liu et al. [85] focused on glycerol and ChCl to produce a DES as a thermal fluid. Since the proportion of 3:1 was specified for the high-quality glycerol/ChCl, all intended nanoparticles (i.e., TiO<sub>2</sub>, Al<sub>2</sub>O<sub>3</sub>, and graphene oxide) were dispersed in the optimum DES, and thus nanofluids were produced. By taking into account the results of zeta potential analysis, proper stability was approved for a week without observing any remarkable participation. It is related to the high viscosity of the base fluid and proper hydrophilicity of the nanoparticles. In addition to viscosity and heat capacity, the thermal conductivity was reported as a key property for all nanofluids, and it was compared to the value of the stated solvent. The dependence of the specific heat capacity was investigated on temperature, and the results indicated that the dispersion of nanoparticles leads to the reduction of specific heat of DES. In this case, the alumina had the highest effect in comparison with others. An increase in the concentration of nanoparticle leads to the enhancement of interaction between solvent and nanoparticles. Thus, the viscosity increases by enhancing volume fraction. Whereas, it becomes negative by raising the temperature. Afterward, it was revealed that temperature had a trivial effect on the optimal thermal conductivity enhancement. Unlike the usual and expected trend, the Al<sub>2</sub>O<sub>3</sub>-DES thermal conductivity has decreased versus the volume fraction. To clarify the reason for happening this phenomenon, <sup>1</sup>H NMR and FT-IR were applied to analyze the mechanism of thermal behavior. This issue revealed that the incident occurred because of the existing hydrogen bond between alumina and glycerol. It restrains both glycerol molecular motion and nanoparticles Brownian motion.

The thermal conductivity of solids is much higher than liquids [98]. Therefore, it is logically expected that suspending nanoparticles into fluids leads to the increment of thermal conductivity. The results of the thermophysical analysis have been reviewed. As a result, it is confirmed that the dispersion of nanoparticles leads to the enhancement of thermal conductivity in DESs. In the majority of cases, it was observed that an increase in temperature and volume fraction leads to the enhancement of thermal conductivity in DES-based nanofluids. The overview of published papers about viscosity indicated that an increase in temperature leads to the decline of viscosity in intended nanofluids, which is similar to the behavior of density.

Fig. 6 and Fig. 7 show the thermal conductivity and viscosity for the representative DESs and DES-based nanofluids as a function of temperature. Almost all the above-described studies have confirmed that the dispersion of nanoparticles improves thermal conductivity in the DESs. By comparing the experimental data of [four] studies, it is revealed that the difference between the total thermal conductivity alterations is



rel: an increase in temperature and the concentration of nanoparticles provide higher thermal conductivity in the prepared nanofluids in comparison with the pure DES. In some cases, the DES-based nanofluids had lower thermal conductivity than the related DES. However, the outcomes were demonstrated that both (DESs and their nanofluids) were significantly superior to commercial cases (VP-1 and Dowtherm-A) [126–128]. Meanwhile, the thermal conductivity of the DES-based nanofluids must be considered for organizing the future theoretical and experimental researches. It is due to the explicit investigation of the effective or ineffective type of HBA and/or HBD (in other words, the H-bond network of DES chemical structure). The efforts should be beneficial to unfold the optimum qualifications for the design of high-quality DES and deep comprehension of the thermal conductivity enhancement in nanofluids based on DES.

As shown in Fig. 7, it is revealed that temperature affects the viscosity of DESs and their nanofluids. The viscosities of both DES and DES-based nanofluids decrease in a similar magnitude. Overall, the results demonstrate that the use of DES as heat transfer fluids is rational, particularly in the form of base liquid for preparing nanofluids.

## 5. Theoretical models for DES-based nanofluids

Both instrumental and theoretical procedures were utilized to detect the changes in profile for thermophysical properties considering disparate effective parameters and experimental conditions. The awareness of characteristics and behavior of DES play an undeniable role in the development of their potential applications. In addition to the many experimental studies represented and discussed in the third section (characterization of DES), this section is principally dealt with a concise review of different theoretical methods for describing the behavior of DESs. According to the literature review, there are a few theoretical studies in the field of DES-based nanofluids. However, many reports have focused on the analysis of the DES behavior and its characteristics, which are constantly updated [99,104–111,129–137]. Several random reports are provided to bring an outlook for the previous studies (Table 5).

The machine-learning techniques are frequently used as a data-driven approach for the theoretical characterization of DESs. In addition to the ease of the implementation, these techniques not only have the capability of learning complex relationships between variables but also provide a high-accuracy prediction for different properties [66,138,139]. These techniques have been applied to estimate the behavior of DES in alkaloids removal [140], glycerol removal [141], and removal of heavy metal as adsorbents [142–146]. To acquire insight into the DES fundamental properties, Adeyemi et al. [147] performed exterminate to measure surface tension, density, conductivity, pH, viscosity, and thermal stability of DESs, including ChCl:monoethanolamine (MEA) (1:6), ChCl:methyldiethanolamine (1:10), and ChCl:diethanolamine

network (ANN), and bagging ANN to predict the density and conductivity of these amine-based DESs. The modified Rackett equation (Eq. 3) [148] is one of the most precise methods for predicting density, and thus it was used for predicting the density of alkanolamine-ChCl DESs.

$$V_s = V' Z_{RA}^{(1-T_r)^{2/7}} \quad (3)$$

$$\text{With } V' = Z_{RA} \frac{RT_c}{P_c} \quad (4) \quad \text{and} \quad Z_{RA} = \left( \frac{V_c P_c}{RT_c} \right)^{\frac{1}{1+(1-T_r)^{2/7}}} \quad (5)$$

where  $V'$  is the characteristic volume,  $T_r$  is the reduced temperature of the saturated liquid,  $Z_{RA}$  is a constant for the mentioned equation, and  $T_c$ ,  $P_c$ , and  $V_c$  are critical temperature, pressure, and volume, respectively. Next, the Lydersen-Joback-Reid equation and Lee-Kesler mixing rule were utilized to calculate the acentric factor, normal boiling point, and critical properties of DESs. Thus, the density was determined for the amine-based DESs. In another modeling method, the multi-layer neural networks were designed by a dataset containing 105 experimental data points. More than half of the available data was set for training networks. Among the several types of the activation and transfer functions, the hyperbolic tangent sigmoid and linear (purelin) were selected as the best functions for input and output layers, respectively. The best design of neural network for both density and conductivity is the neural architecture with a set of neurons of 6, 10, and 1 as input layer (containing mole fraction of each component formed DES, the molecular weight of the DESs, and temperature), hidden layer, and output layer, respectively. The bagging ANN is based on ensemble learning. Thus, an ensemble of conventional ANN is selected, and it is inspired by declining deviations and reinforcing the correct decisions. Three resampling sizes of 10, 20, and 30 were studied. Statistical descriptors were calculated and analyzed to define the creditability of the developed models. The statistical descriptors were comprised of geometric mean bias (MG), normalized mean square error (NMSE), index of agreement (IA), average absolute relative deviation (AARD), fractional bias (FB), as well as geometric variance (VG), and regression coefficient ( $R^2$ ). The evaluation outcomes confirmed that bagging ANN is the most accurate method in comparison with other methods. Also, the best prediction was achieved by a size of 30 ( $n=30$ ). The ChCl-DEA density was predicted by the least AARD values of 5.81% and 0.02% using the modified Rackett and bagging ANN methods, respectively. Similar to the density, thermal conductivity was predicted by developing appropriate networks, and the statistical analysis proved that the prediction of bagging ANN had better validity than ANN. Moreover, the highest and lowest conductivities were observed for ChCl-MEA (1:6) and ChCl-DEA (1:6), respectively.

of new materials, molecular simulation techniques based on statistical mechanics are considered as one of the efficient alternatives for predicting molecular interactions, and physicochemical properties of pure compounds and their mixtures [149]. Sun et al. [150] and Perkins et al. [151] firstly developed molecular dynamic (MD) simulations to investigate the main inter-molecular interactions in ChCl-based DES. Atilhan and Aparicio [152] performed a molecular dynamics (MD) study on DESs. They investigated the solvation and aggregation process of metal nanoparticles (gold, silver, palladium, platinum, and nickel) considering geometry, type, and size of nanoparticles together with DES characteristics. The MD simulations were implemented in the ACEMD program [153]. Also, the metal nanoparticles were made using openMD software. The effects of nanoparticles' shape were also investigated and the results demonstrated that nanoparticles in spherical shape were more competent solvation than icosahedral. Accordingly, their MD survey exhibited that DES could act as a stabilizer and prevent the aggregation of nanoparticles. Also, it solvates various types of nanoparticles in an effective manner. Furthermore, the DESs as a convenient medium generate a stable solution for nanoparticles with monitored size.

There is a lack of adequate investigations in the area of developing appropriate modeling approaches to predict the properties of DES-based nanofluids. Therefore, it is necessary to solve this issue. Osama et al. [118] conducted a study to compare the thermal conductivity of graphene oxide-DES nanofluid with theoretical models. The thermal conductivity was estimated by using Kumar [120] and Rashmi's models [119]. These models are represented as follows:

$$\text{Rashmi's model} \quad k_{\text{eff}} = k_{\text{bf}} \left[ 1 + \frac{k_p^{2\varphi(a_p+1)p}}{a_p l_p} \right] + \frac{C\varphi(T-T_0)}{a_{\text{bf}}^2 l_{\text{bf}}^2 \mu_{\text{bf}}} \ln \left( \frac{l_p}{d_p} \right) \quad (4)$$

$$\text{Kumar's model} \quad k_{\text{eff}} = k_{\text{bf}} + c \frac{2k_B T \varphi a_{\text{bf}}}{\pi \mu d_p^2 (1-\varphi)} \quad (5)$$

where  $k$  is the thermal conductivity coefficient,  $\varphi$  is volume fraction,  $a$  referred to as the nanoparticle/liquid molecule radius,  $l$  is particle length,  $\mu$  is fluid viscosity,  $d$  is the diameter of nanoparticles,  $k_B$  is the constant of Boltzmann, and  $n$ ,  $c$ , and  $T_0$  are constant values. Subscripts of eff, p, and bf refer to the effective property of nanofluids, nanoparticle (graphene oxide), and the base fluid (the DESs composed of EG and MTPB in 3:1 and 5:1 molar ratios), respectively. Although the shape of nanoparticles in Rashmi's model is assumed spherical and there is not a factor for the representation of the shape considering Brownian motion [119]. In other words, the stationary particle and moving particle models are elements that compose the Kumar's model [154]. The predictability of the above-mentioned models was evaluated by the experimental findings of thermal conductivity in the prepared nanofluids. The prediction error was determined for equations (4) and (5) by computing the percentage deviation from the real thermal conductivity values. In this case,

yield of theoretical models for the prediction of thermal conductivity, Osama et al. [118] modified equation (5) and designed a new equation, namely Kumar's modified model. This model is formulated by Equation (6), and it is used to improve predictability.

$$\text{Kumar's modified model} \quad k_{\text{eff}} = k_{\text{bf}} + \left( \frac{\varphi}{(1-\varphi)} \right)^n TC_0 \quad (6)$$

$$C_0 = \frac{\frac{2(a_p+1)p}{a_p^2}}{\left( \frac{3}{a_{\text{bf}}} \right)}$$

Finally in report [9], it was found that the predictive power of studied models was in this order: Kumar's modified > Rashmi > Kumar. The n power variable was a function of temperature, and it was changed considering the molar ratio of DES components.

It is worth to be referred to the excellent recent review by Ismail et al. [155] on the perspectives of thermodynamic modeling of DES. They outlined a summary of the recent studies and generic instructions for choosing the modeling techniques.

## 6. Conclusions

The contribution of the global research community should be strengthened to correct and promote heat transfer applications. This implies that the scientific community should pay a great deal of attention to the development of the applications and performance of green solvents in heat transfer. A promising economic alternative is associated with the deep eutectic solvents, which are admixtures of an organic compound and salt with a notably decreased melting point over the real ingredients. By taking into consideration the overlap shared by these two classes (i.e., IL and DES), it should be emphasized that the DESs have a lighter ecological footprint and better suited in scale-up. Besides, the DESs are far facilitated to be prepared by a simple mixing method without generating any waste in the formation process. To derive the advantage of the green-based DESs as designable solvents, the broad array of the potential combinations of components creates possible targeted syntheses for the green-based DESs with special properties in the intended applications. It was mentioned that most DESs possess high viscosity, which shows a negative change in high temperatures. Thus, the development of DES must be considered with less viscosity. Fortunately, most heat transfer liquids should be used in high-temperature media. Therefore, this could be a supportive option. Furthermore, although water is the best choice in scientific and industrial purposes regard to availability, abundance, and its outstanding thermophysical properties; meanwhile there is need to spread awareness on ways to save water in industries by reducing its consumption. Using less water creates less wastewater, which in turn uses less energy and costs less money. In seek for alternative options to reduce using of water

and planning, a well-designed DES can reduce water consumption.

This paper provides a snapshot of the exciting progress made over the last years in the area of employing DESs and their role of base fluids for preparing nanofluids. The reviewed literature indicated that the thermal conductivity of the nanofluids increases when the temperature and volume fraction increase, except in some cases in which an increase in the volume fraction leads to the enhancement of thermal conductivity. It is due to the unique hydrogen interactions between the nanoparticle and DES. A portion of the contribution of this study was devoted to the review of the preparation process for the DES, DES-based nanofluids, and effective methods for increasing the stability of nanofluids. Furthermore, some aspects of their structures and properties were discussed and a roadmap was offered for the future potential usages of the DES together with their existing applications such as shape-controlled nanoparticle synthesis, removing heavy metals from water, extraction of bioactive substances, and dye-sensitized solar cells. The diversity of the DESs makes them a high-quality potential candidate for applying in many other fields. There are a few studies that investigated the effect of HBD/HBA nature on the thermal conductivity of the DES and presented an overview to make an optimum decision for choosing the best option for the DES as heat transfer fluid. It is essential to develop more investigations for clarifying the detail of potential applications of these promising fluids. The findings of this study revealed that the researches on developments and potential applications of the DESs are still far from enough. It is necessary to first elucidate the role of operative parameters in the improvement of DES thermophysical properties and the construction of new DESs based on theoretical approaches. Thus, the options with more desirable features are designated for discovering the eco-friendly option in heat transport. It is not currently possible to claim that deep eutectic solvents are the best selection for the heat transfer fluid, however, it gave promising results. Finally, this issue requires further studies and attention from the scientific community to become compatible with nature by developing green choices.

### **Conflict of interest**

None declared.

AARD	Average absolute relative deviation	IL	Ionic liquid
ANN	Artificial neural network	MD	Molecular dynamic simulation
bf	Base fluid	MEA	Monoethanolamine
BTPC	Benzyltriphenyl phosphonium chloride	MG	Geometric mean bias
ChCl	Choline chloride	MIP	Molecular imprinted polymer
C-MAS-NMR	<sup>13</sup> C-magic angle spinning-NMR	MPTMS	3-mercaptopropyl trimethoxy silane
C-NMR	Carbon nuclear magnetic resonance	MTPB	Methyl-triphenylphosphonium-bromide
CNT	Carbon nanotube	MWCNT	Multi-wall carbon nanotube
cP	Centi poise (1P = 1g.cm <sup>-1</sup> .s <sup>-1</sup> )	N	Nano particle
CSP	Concentrated solar power	NADES	Natural deep eutectic solvent
DAC	N,N diethylethanolammium chloride	Nf	Nanofluid
DBSA-PANI	Dodecyl benzene sulfonic acid doped polyaniline	NMSE	Normalized mean square error
DEA	Diethanolamine	R <sup>2</sup>	Regression coefficient
DES	Deep eutectic solvent	Re	Reynold number
DNA	Deoxyribonucleic acid	rpm	Rate per minute
DP	2-butoxy-3,4-dihydropyran	SEM	Scanning electron microscopy
DSC	Differential scanning calorimetry	TBAB	Tetra-n-butyl ammonium bromide
EG	Ethylene glycol	TEG	Triethylene glycol
FB	Fractional bias	TEM	Transmission electron microscopy
FT-IR	Fourier-transform infrared spectroscopy	TEOS	Tetraethyl orthosilicate
HBA	Hydrogen bond acceptor	TGA	Thermal gravimetric analysis
HBD	Hydrogen bond donor	UV	Ultra violet spectroscopy
H-NMR	Proton nuclear magnetic resonance	VG	Geometric variance
IA	Index of agreement	XPS	X-ray photoelectron spectroscopy
IEP	Isoelectric point	XRD	X-ray powder diffraction

## References

- [1] E. Pop, Energy dissipation and transport in nanoscale devices, *Nano Res.* 3 (2010) 147–169.
- [2] M. Hernaiz, V. Alonso, P. Estelle, Z. Wu, B. Sunden, L. Doretto, S. Mancin, N. Cobanoglu, Z.H. Karadeniz, N. Garmendia, M. Lasheras-Zubiarte, L. Hernandez Lopez, R. Mondragon, R. Martinez-Cuenca, S. Barison, A. Kujawska, A. Turgut, A. Amigo, G. Huminic, A. Huminic, M.-R. Kalus, K.-G. Schroth, M.H. Buschmann, The contact angle of nanofluids as thermophysical property, *J. Colloid Interface Sci.* 547 (2019) 393–406. doi:10.1016/j.jcis.2019.04.007.
- [3] S.U.S. Choi, J.A. Eastman, *Enhancing thermal conductivity of fluids with nanoparticles*, Argonne National Lab., IL (United States), 1995.
- [4] B. Ma, D. Banerjee, Chapter 6 A Review of Nanofluid Synthesis, 2018. doi:10.1007/978-3-319-

- [5] N. Sezer, M.A. Atieh, M. Koç, A comprehensive review on synthesis, stability, thermophysical properties, and characterization of nanofluids, *Powder Technol.* 344 (2019) 404–431. doi:10.1016/j.powtec.2018.12.016.
- [6] A. Asadi, S. Aberoumand, A. Moradikazerouni, F. Pourfattah, P. Estellé, O. Mahian, S. Wongwises, H.M. Nguyen, A. Arabkoohsar, Recent advances in preparation methods and thermophysical properties of oil-based nanofluids: A state-of-the-art review, 352 (2019) 209–226. doi:10.1016/j.powtec.2019.04.054.
- [7] H. Khodadadi, S. Aghakhani, H. Majd, R. Kalbasi, S. Wongwises, A comprehensive review on rheological behavior of mono and hybrid nanofluids: Effective parameters and predictive correlations, *Int. J. Heat Mass Transf.* 127 (2018) 997–1012. doi:10.1016/j.ijheatmasstransfer.2018.07.103.
- [8] S. Akilu, K. V Sharma, A. Tesfamichael, R. Mamat, A review of thermophysical properties of water based composite nanofluids, *Renew. Sustain. Energy Rev.* 66 (2016) 654–678. doi:10.1016/j.rser.2016.08.036.
- [9] N. Ali, J.A. Teixeira, A. Addali, A Review on Nanofluids: Fabrication, Stability, and Thermophysical Properties, *J. Nanomater.* 2018 (2018) 1–33. doi:10.1155/2018/6978130.
- [10] W.H. Azmi, K. V Sharma, R. Mamat, G. Naja, M.S. Mohamad, The enhancement of effective thermal conductivity and effective dynamic viscosity of nanofluids – A review, 53 (2016) 1046–1058. doi:10.1016/j.rser.2015.09.081.
- [11] P.T. Anastas, M.M. Kirchhoff, Origins, current status, and future challenges of green chemistry, *Acc. Chem. Res.* 35 (2002) 685–694.
- [12] P.T. Anastas, J.C. Warner, Oxford University Press, Oxford, 1998, *Green Chem.* (1999) G21.
- [13] F.M. Kerton, Solvent Systems for Sustainable Chemistry, *Encycl. Inorg. Bioinorg. Chem.* (2011) 1–17. doi:10.1002/9781119951438.eibc2417.
- [14] R. Hayes, G.G. Warr, R. Atkin, Structure and Nanostructure in Ionic Liquids, *Chem. Rev.* 115 (2006) 6357–6426. doi:10.1021/cr500411q.
- [15] V.A. Parsegian, Van der Waals forces: a handbook for biologists, chemists, engineers, and physicists, Cambridge University Press, 2005.

- modified graphene/ionic liquid nanofluids with excellent dispersion stability, *Sol. Energy Mater. Sol. Cells*. 170 (2017) 219–232.
- [17] K. Ghandi, A review of ionic liquids, their limits and applications, *Green Sustain. Chem.* 2014 (2014).
- [18] M. Amde, J.-F. Liu, L. Pang, Environmental application, fate, effects, and concerns of ionic liquids: a review, *Environ. Sci. Technol.* 49 (2015) 12611–12627.
- [19] A. Hosseinghorbani, M. Moza, G. Pazuki, Application of graphene oxide Ionano fluid as a superior heat transfer fluid in concentrated solar power plants, *Int. Commun. Heat Mass Transf.* 111 (2020) 104450. doi:10.1016/j.icheatmasstransfer.2019.104450.
- [20] N.J. Bridges, A.E. Visser, E.B. Fox, Potential of Nanoparticle-Enhanced Ionic Liquids ( NEILs ) as Advanced Heat-Transfer Fluids, (2011) 4862–4864.
- [21] A.E. Visser, N.J. Bridges, B.L. Garcia-diaz, J.R. Gray, E.B. Fox, S. Carolina, Al<sub>2</sub>O<sub>3</sub>-Based Nanoparticle-Enhanced Ionic Liquids (NEILs) for advanced heat transfer fluids, *Ion. Liq. Sci. Appl. Am. Chem. Soc.* (2012) 259–270.
- [22] B. Wang, X. Wang, W. Lou, J. Hao, Ionic liquid-based stable nanofluids containing gold nanoparticles, *J. Colloid Interface Sci.* 352 (2011) 5–14.
- [23] M.P. Shevelyova, Y.U. Paulechko, G.J. Kabo, A. V Blokhin, A.G. Kabo, T.M. Gubarevich, Physicochemical Properties of Imidazolium-Based Ionic Nanofluids: Density, Heat Capacity, and Enthalpy of Formation, *J. Phys. Chem. B*. 117 (2013) 4782–4790.
- [24] M.G. Freire, C.M.S.S. Neves, I.M. Marrucho, A.P. Coutinho, Hydrolysis of Tetrafluoroborate and Hexafluorophosphate Counter Ions in Imidazolium-Based Ionic Liquids †, 2 (2010) 3744–3749.
- [25] R.P. Swatloski, J.D. Holbrey, R.D. Rogers, Ionic liquids are not always green: hydrolysis of 1-butyl-3-methylimidazolium hexafluorophosphate, (2003) 361–363. doi:10.1039/b304400a.
- [26] A. Adriana, S.M.S. Murshed, A review on development of ionic liquid based nanofluids and their heat transfer behavior, *Renew. Sustain. Energy Rev.* 91 (2018) 584–599. doi:10.1016/j.rser.2018.04.021.
- [27] S. Faisal, M. Khalid, W. Rashmi, A. Chan, K. Shahbaz, Recent progress in solar thermal energy storage using nanomaterials, *Renew. Sustain. Energy Rev.* 67 (2017) 450–460. doi:10.1016/j.rser.2016.09.034.



doi:10.1007/s41061-017-0148-1.

- [29] K. Shahbaz, F.S. Mjalli, M.A. Hashim, I.M. AlNashef, Prediction of deep eutectic solvents densities at different temperatures, *Thermochim. Acta.* 515 (2011) 67–72.
- [30] E.L. Smith, A.P. Abbott, K.S. Ryder, Deep Eutectic Solvents (DESs) and Their Applications, *Chem. Rev.* 114 (2014) 11060–11082. doi:10.1021/cr300162p.
- [31] U.D. De Qui, Chapter 5 - Deep eutectic solvents, Elsevier Inc., 2020. doi:10.1016/B978-0-12-817386-2.00005-6.
- [32] A.P. Abbott, D. Boothby, G. Capper, D.L. Davies, R.K. Rasheed, Deep eutectic solvents formed between choline chloride and carboxylic acids: versatile alternatives to ionic liquids, *J. Am. Chem. Soc.* 126 (2004) 9142–9147.
- [33] Q. Zhang, K. De Oliveira Vigier, S. Royer, F. Jérôme, Deep eutectic solvents: Syntheses, properties and applications, *Chem. Soc. Rev.* 41 (2012) 7108–7146. doi:10.1039/c2cs35178a.
- [34] B. Wang, L. Qin, T. Mu, Z. Xue, G. Gao, Are ionic liquids chemically stable?, *Chem. Rev.* 117 (2017) 7113–7131.
- [35] A. Abo-Hamad, M. Hayyan, M.A.H. AlSaadi, M.A. Hashim, Potential applications of deep eutectic solvents in nanotechnology, *Chem. Eng. J.* 273 (2015) 551–567. doi:10.1016/j.cej.2015.03.091.
- [36] D. V Wagle, H. Zhao, G.A. Baker, Deep eutectic solvents: sustainable media for nanoscale and functional materials, *Acc. Chem. Res.* 47 (2014) 2299–2308.
- [37] D.Z. Troter, Z.B. Tođorović, D.R. Đokić-Stojanović, O.S. Stamenković, V.B. Veljković, Application of ionic liquids and deep eutectic solvents in biodiesel production: A review, *Renew. Sustain. Energy Rev.* 61 (2016) 473–500.
- [38] D.A. Alonso, A. Baeza, R. Chinchilla, G. Guillena, I.M. Pastor, D.J. Ramón, Deep eutectic solvents: the organic reaction medium of the century, *European J. Org. Chem.* 2016 (2016) 612–632.
- [39] X. Li, K.H. Row, Development of deep eutectic solvents applied in extraction and separation, *J. Sep. Sci.* 39 (2016) 3505–3520.
- [40] R. Haghbakhsh, M. Taherzadeh, A.R.C. Duarte, S. Raeissi, A general model for the surface tensions of deep eutectic solvents, *J. Mol. Liq.* (2020) 112972. doi:10.1016/j.molliq.2020.112972.
- [41] W. Bi, M. Tian, K.H. Row, Evaluation of alcohol-based deep eutectic solvent in extraction and

- (2013) 22–30.
- [42] Q. Cui, X. Peng, X.-H. Yao, Z.-F. Wei, M. Luo, W. Wang, C.-J. Zhao, Y.-J. Fu, Y.-G. Zu, Deep eutectic solvent-based microwave-assisted extraction of genistin, genistein and apigenin from pigeon pea roots, *Sep. Purif. Technol.* 150 (2015) 63–72.
- [43] L. Piemontese, F.M. Perna, A. Logrieco, V. Capriati, M. Solfrizzo, Deep eutectic solvents as novel and effective extraction media for quantitative determination of ochratoxin A in wheat and derived products, *Molecules*. 22 (2017) 121.
- [44] A. Shishov, A. Bulatov, M. Locatelli, S. Carradori, V. Andrich, Application of deep eutectic solvents in analytical chemistry. A review, *Microchem. J.* 135 (2017) 33–53  
doi:10.1016/j.microc.2017.07.015.
- [45] R. Bernasconi, G. Panzeri, A. Accogli, F. Liberale, L. Nobili, L. Magagnin, Electrodeposition from deep eutectic solvents, *Prog. Dev. Ion. Liq.* (2017) 235–261.
- [46] A.P. Abbott, A. Ballantyne, R.C. Harris, J.A. Junge, K.S. Ryder, G. Forrest, A comparative study of nickel electrodeposition using deep eutectic solvents and aqueous solutions, *Electrochim. Acta.* 176 (2015) 718–726.
- [47] J. Vijayakumar, S. Mohan, S.A. Kurian, S.R. Suseendiran, S. Pavithra, Electrodeposition of Ni–Co–Sn alloy from choline chloride-based deep eutectic solvent and characterization as cathode for hydrogen evolution in alkaline solution, *Int. J. Hydrogen Energy.* 38 (2013) 10208–10214.
- [48] L. Anicai, A. Petica, S. Costarelli, P. Prioteasa, T. Visan, Electrodeposition of Sn and NiSn alloys coatings using choline chloride based ionic liquids—Evaluation of corrosion behavior, *Electrochim. Acta.* 114 (2013) 868–877.
- [49] M.C. Gutiérrez, D. Carriazo, A. Tamayo, R. Jiménez, F. Picó, J.M. Rojo, M.L. Ferrer, F. del Monte, Deep-Eutectic-Solvent-Assisted Synthesis of Hierarchical Carbon Electrodes Exhibiting Capacitance Retention at High Current Densities, *Chem. Eur. J.* 17 (2011) 10533–10537.
- [50] T. Křížek, M. Bursová, R. Horsley, M. Kuchař, P. Tůma, Menthol-based hydrophobic deep eutectic solvents: Towards greener and efficient extraction of phytocannabinoids, *J. Clean. Prod.* 193 (2018) 391–396. doi:10.1016/j.jclepro.2018.05.080.
- [51] Q. Cui, J. Liu, L. Wang, Y. Kang, Y. Meng, J. Jiao, Y. Fu, Sustainable deep eutectic solvents preparation and their efficiency in extraction and enrichment of main bioactive flavonoids from sea

- [52] N. Nia Noorae, M.R. Hadjmohammadi, The application of three-phase solvent bar microextraction based on a deep eutectic solvent coupled with high-performance liquid chromatography for the determination of flavonoids from vegetable and fruit juice samples, *Anal. Methods*. (2019) 5134–5141. doi:10.1039/c9ay01704f.
- [53] S. Saadi, M. Abdulhakim, W. Zurina, Review on heavy metal adsorption processes by carbon nanotubes, *J. Clean. Technol.* 230 (2019) 783–793. doi:10.1016/j.jclepro.2019.05.154.
- [54] H.-R. Jhong, D.S.-H. Wong, C.-C. Wan, Y.-Y. Wang, T.-C. Wei, A novel deep eutectic solvent-based ionic liquid used as electrolyte for dye-sensitized solar cells, *Electrochem. Commun.* 11 (2009) 209–211.
- [55] Y. Marcus, *Deep Eutectic Solvents*, Springer Nature Switzerland, 2019. doi:10.1007/978-3-030-00608-2\_4.
- [56] L.I.N. Tomé, V. Baião, W. da Silva, C.M.A. Brett, Deep eutectic solvents for the production and application of new materials, *Appl. Mater. Today* 10 (2018) 30–50. doi:10.1016/j.apmt.2017.11.005.
- [57] Y. Cui, C. Li, J. Yin, S. Li, Y. Jia, M. Bao, Design, synthesis and properties of acidic deep eutectic solvents based on choline chloride, *J. Mol. Liq.* 236 (2017) 338–343.
- [58] M. Jablonský, A. Škulcová, J. Šima, Use of deep eutectic solvents in polymer chemistry—a review, *Molecules*. 24 (2019) 1–33. doi:10.3390/molecules24213978.
- [59] H. Qin, X. Hu, J. Wang, H. Cheng, L. Chen, Z. Qi, Overview of acidic deep eutectic solvents on synthesis, properties and applications, *Green Energy Environ.* 5 (2020) 8–21.
- [60] Y. Dai, R. Verpoorte, Y.H. Choi, Natural deep eutectic solvents providing enhanced stability of natural colorants from safflower (*Carthamus tinctorius*), *Food Chem.* 159 (2014) 116–121.
- [61] Y. Dai, G.-J. Witkamp, R. Verpoorte, Y.H. Choi, Natural deep eutectic solvents as a new extraction media for phenolic metabolites in *Carthamus tinctorius* L., *Anal. Chem.* 85 (2013) 6272–6278.
- [62] L.K. Savi, D. Carpine, N. Waszczynskij, R.H. Ribani, C. Windson Isidoro Haminiuk, Influence of temperature, water content and type of organic acid on the formation, stability and properties of functional natural deep eutectic solvents, *Fluid Phase Equilib.* 488 (2019) 40–47. doi:10.1016/j.fluid.2019.01.025.
- [63] A.P. Abbott, G. Capper, D.L. Davies, R.K. Rasheed, V. Tambyrajah, Novel solvent properties of

- [64] T. Aissaoui, Y. Benguerba, M.K. AlOmar, I.M. AlNashef, Computational investigation of the microstructural characteristics and physical properties of glycerol-based deep eutectic solvents, *J. Mol. Model.* 23 (2017) 277.
- [65] Y. Dai, J. Van Spronsen, G. Witkamp, Natural deep eutectic solvents as new potential media for green technology, *Anal. Chim. Acta.* 766 (2013) 61–68. doi:10.1016/j.aca.2012.12.019.
- [66] K. Shahbaz, S. Baroutian, F.S. Mjalli, M.A. Hashim, I.M. AlNashef, Densities of ammonium and phosphonium based deep eutectic solvents: Prediction using artificial intelligence and group contribution techniques, *Thermochim. Acta.* 527 (2012) 59–66.
- [67] C. Florindo, F.S. Oliveira, L.P.N. Rebelo, A.M. Fernandes, I.M. Marrucho, Insights into the Synthesis and Properties of Deep Eutectic Solvents Based on Cholinium Chloride and Carboxylic Acids, (2014).
- [68] M.A. Kareem, F.S. Mjalli, M.A. Hashim, I.M. AlNashef, Phosphonium-Based Ionic Liquids Analogues and Their Physical Properties, *J. Chem. Eng. Data.* 55 (2010) 4632–4637.
- [69] P.B. Sánchez, B. González, J. Salgado, J. Losa Parajó, Á. Domínguez, Physical properties of seven deep eutectic solvents based on L-proline or betaine, *J. Chem. Thermodyn.* 131 (2019) 517–523. doi:10.1016/j.jct.2018.12.017.
- [70] F. Cardellini, M. Tiecco, R. Germani, G. Cardinali, L. Corte, L. Roscini, N. Spreti, Novel zwitterionic deep eutectic solvents from trimethylglycine and carboxylic acids: characterization of their properties and their toxicity †, *RSC Adv.* 4 (2014) 55990–56002. doi:10.1039/C4RA10628H.
- [71] X. Liu, B. Gao, Y. Jiang, N. Ai, D. Deng, Solubilities and Thermodynamic Properties of Carbon Dioxide in Guaiacol-Based Deep Eutectic Solvents, *J. Chem. Eng. Data.* 62 (2017) 1448–1455. doi:10.1021/acs.jced.6b01013.
- [72] F.S. Mjalli, J. Naser, B. Jibril, V. Alizadeh, Z. Gano, Tetrabutylammonium Chloride Based Ionic Liquid Analogues and Their Physical Properties, *J. Chem. Eng. Data.* 59 (2014) 2242–2251.
- [73] D. Deng, X. Liu, B. Gao, Physicochemical Properties and Investigation ofazole-based deep eutectic solvents as efficient and reversible SO<sub>2</sub> absorbents Physicochemical Properties and Investigation of Azole-Based Deep Eutectic Solvents as Efficient and Reversible SO<sub>2</sub> Absorbents, *Ind. Eng. Chem. Res.* 56 (2017) 13850–13856. doi:10.1021/acs.iecr.7b02478.
- [74] T. Aissaoui, I.M. AlNashef, U.A. Qureshi, Y. Benguerba, Potential applications of deep eutectic

- [75] Z. Maugeri, P.D. de María, Novel choline-chloride-based deep-eutectic-solvents with renewable hydrogen bond donors: levulinic acid and sugar-based polyols, *Rsc Adv.* 2 (2012) 421–425.
- [76] X. Li, Y.R. Lee, K.H. Row, Synthesis of mesoporous siliceous materials in choline chloride deep eutectic solvents and the application of these materials to high-performance size exclusion chromatography, *Chromatographia.* 79 (2016) 375–382.
- [77] Y. Marcus, The entropy of deep eutectic solvent formation, *Entropy.* 20 (2018) 524.
- [78] X. Li, J. Choi, W.-S. Ahn, K.H. Row, Preparation and application of porous materials based on deep eutectic solvents, *Crit. Rev. Anal. Chem.* 48 (2018) 73–85.
- [79] B. Tang, H. Zhang, K.H. Row, Application of deep eutectic solvents in the extraction and separation of target compounds from various samples, *J. Sep. Sci.* 38 (2015) 1053–1064.
- [80] A. Ounissi, Y. Benguerba, N. Ouddai, Theoretical investigation on structural and physicochemical properties of some ionic liquids, *Comput. Theor. Chem.* 1092 (2016) 68–73.
- [81] X. Li, K. Ho, Separation of Polysaccharides by SEC Utilizing Deep Eutectic Solvent Modified Mesoporous Siliceous Materials, *Chromatographia.* (2017). doi:10.1007/s10337-017-3336-9.
- [82] R.K. Ibrahim, M. Hayyan, M.A. AlSaddi, S. Ibrahim, A. Hayyan, M.A. Hashim, Physical properties of ethylene glycol-based deep eutectic solvents, *J. Mol. Liq.* 276 (2019) 794–800. doi:10.1016/j.molliq.2018.12.032.
- [83] Y. Hou, Y. Gu, S. Zhang, F. Yang, H. Ding, Y. Shan, Novel binary eutectic mixtures based on imidazole, *J. Mol. Liq.* 143 (2008) 154–159.
- [84] D. Carriazo, M. a. C. Gutiérrez, ML Ferrer and F. del Monte, *Chem. Mater.* 22 (2010) 6146–6152.
- [85] C. Liu, H. Fang, Y. Qiao, J. Zhao, Z. Rao, Properties and heat transfer mechanistic study of glycerol/choline chloride deep eutectic solvents based nanofluids, *Int. J. Heat Mass Transf.* 138 (2019) 690–698. doi:10.1016/j.ijheatmasstransfer.2019.04.090.
- [86] P.K. Naik, S. Paul, T. Banerjee, Physicochemical Properties and Molecular Dynamics Simulations of Phosphonium and Ammonium Based Deep Eutectic Solvents, *J. Solution Chem.* 48 (2019) 1046–1065. doi:10.1007/s10953-019-00903-0.
- [87] W. Chen, X. Bai, Z. Xue, H. Mou, J. Chen, Z. Liu, T. Mu, The formation and physicochemical properties of PEGylated deep eutectic solvents, *New J. Chem.* 43 (2019) 8804–8810.

- [88] A. Abri, N. Babajani, A.M. Zonouz, H. Shekaari, Spectral and thermophysical properties of some novel deep eutectic solvent based on l-menthol and their mixtures with ethanol, *J. Mol. Liq.* 285 (2019) 477–487. doi:10.1016/j.molliq.2019.04.001.
- [89] W. Yu, H. Xie, A review on nanofluids: preparation, stability mechanisms, and applications, *J. Nanomater.* 2012 (2012).
- [90] A. Ghadimi, R. Saidur, H.S.C. Metselaar, A review of nanofluid stability properties and characterization in stationary conditions, *Int. J. Heat Mass Transf.* 54 (2011) 4051–4068. doi:10.1016/j.ijheatmasstransfer.2011.04.014.
- [91] S.K. Sharma, S.M. Gupta, Preparation and evaluation of stable nanofluids for heat transfer application: a review, *Exp. Therm. Fluid Sci.* 79 (2016) 202–212.
- [92] J.-C. Chou, L.P. Liao, Study on pH at the point of zero charge of TiO<sub>2</sub> pH ion-sensitive field effect transistor made by the sputtering method, *Thin Solid Films.* 476 (2005) 157–161.
- [93] A.K. Gupta, S. Wells, Surface-modified superparamagnetic nanoparticles for drug delivery: preparation, characterization, and cytotoxicity studies, *IEEE Trans. Nanobioscience.* 3 (2004) 66–73.
- [94] A. Asadi, F. Pourfattah, I. Miklós Szilágyi, M. Afrand, G. Żyła, H. Seon Ahn, S. Wongwises, H. Minh Nguyen, A. Arabkoohsar, O. Mahian, Effect of sonication characteristics on stability, thermophysical properties, and heat transfer of nanofluids: A comprehensive review, *Ultrason. Sonochem.* 58 (2019). doi:10.1016/j.ultsonch.2019.104701.
- [95] W. Wang, Z. Wu, B. Li, B. Sundé, A review on molten-salt-based and ionic-liquid-based nanofluids for medium-to-high temperature heat transfer, *J. Therm. Anal. Calorim.* 0123456789 (2018). doi:10.1007/s10973-018-7765-y.
- [96] C. Liu, H. Fang, X. Liu, B. Xu, Z. Rao, Novel silica filled deep eutectic solvent based nanofluids for energy transportation, *Sustain. Chem. Eng.* (2019). doi:10.1021/acssuschemeng.9b06179.
- [97] M.U. Sajid, H.M. Ali, Thermal conductivity of hybrid nanofluids: A critical review, *Int. J. Heat Mass Transf.* 126 (2018) 211–234. doi:10.1016/j.ijheatmasstransfer.2018.05.021.
- [98] O. Mahian, L. Kolsi, M. Amani, P. Estellé, G. Ahmadi, C. Kleinstreuer, J.S. Marshall, M. Siavashi, R.A. Taylor, H. Niazmand, S. Wongwises, T. Hayat, A. Kolanjiyil, A. Kasaeian, I. Pop, Recent advances in modeling and simulation of nanofluid flows-Part I: Fundamentals and theory, *Phys. Rep.* 790 (2019) 1–48. doi:10.1016/j.physrep.2018.11.004.

- (2019) 1–8. doi:10.1007/s10973-019-09000-2.
- [100] P. Dehury, J. Singh, T. Banerjee, Thermophysical and Forced Convection Studies on ( Alumina + Menthol ) -Based Deep Eutectic Solvents for Their Use as a Heat Transfer Fluid, *ACS Omega*. 3 (2018) 18016–18027. doi:10.1021/acsomega.8b02661.
- [101] E.L. Smith, A.P. Abbott, K.S. Ryder, Deep eutectic solvents (DESs) and their applications, *Chem. Rev.* 114 (2014) 11060–11082.
- [102] Y. Dai, G.-J. Witkamp, R. Verpoorte, Y.H. Choi, Tailoring properties of natural deep eutectic solvents with water to facilitate their applications, *Food Chem.* 167 (2015) 14–19.
- [103] O.S. Hammond, D.T. Bowron, K.J. Edler, The effect of water upon deep eutectic solvent nanostructure: An unusual transition from ionic mixture to aqueous solution, *Angew. Chemie Int. Ed.* 56 (2017) 9782–9785.
- [104] D. Lapeña, L. Lomba, M. Artal, C. Lafuente, B. Giner, Thermophysical characterization of the deep eutectic solvent choline chloride: ethylene glycol and one of its mixtures with water, *Fluid Phase Equilib.* 492 (2019) 1–9.
- [105] H.Z. Su, J.M. Yin, Q.S. Liu, C.P. Li, Properties of four deep eutectic solvents: Density, electrical conductivity, dynamic viscosity and refractive index, *Acta Physico-Chimica Sin.* 31 (2015) 1468–1473. doi:10.3866/PKU.WHXB201506111.
- [106] J. Zhu, K. Yu, Y. Zhu, R. Zhu, F. Ye, N. Song, Y. Xu, Physicochemical properties of deep eutectic solvents formed by choline chloride and phenolic compounds at T=(293.15 to 333.15) K: The influence of electronic effect of substitution group, *J. Mol. Liq.* 232 (2017) 182–187. doi:10.1016/j.molliq.2017.02.071.
- [107] D. Lapeña, F. Bergua, L. Lomba, B. Giner, C. Lafuente, A comprehensive study of the thermophysical properties of reline and hydrated reline, *J. Mol. Liq.* (2020) 112679. doi:10.1016/j.molliq.2020.112679.
- [108] A. Škulcová, V. Majová, T. Dubaj, M. Jablonský, Physical properties and thermal behavior of novel ternary green solvents, *J. Mol. Liq.* 287 (2019) 110991. doi:10.1016/j.molliq.2019.110991.
- [109] M.A. Sedghamiz, S. Raeissi, Physical properties of deep eutectic solvents formed by the sodium halide salts and ethylene glycol, and their mixtures with water, *J. Mol. Liq.* 269 (2018) 694–702. doi:10.1016/j.molliq.2018.08.045.

- [11] ammonium chloride-glycerol or ethylene glycol deep eutectic solvents and their aqueous solutions, *J. Chem. Thermodyn.* 65 (2013) 65–72. doi:10.1016/j.jct.2013.05.041.
- [111] P.B. Sánchez, B. González, J. Salgado, J. José, Á. Domínguez, Physical properties of seven deep eutectic solvents based on L -proline or betaine, *131 (2019) 517–523.* doi:10.1016/j.jct.2018.12.017.
- [112] A.P. Abbott, G. Capper, S. Gray, Design of improved deep eutectic solvents using hole theory, *Chemphyschem a Eur. J. Chem. Phys. Phys. Chem.* 7 (2006) 803–806.
- [113] Y.K. Fang, M. Osama, W. Rashmi, K. Shahbaz, M. Khalid, F.S. Mjalli, M.M. Farid, Synthesis and thermo-physical properties of deep eutectic solvent-based graphene nanofluids, *Nanotechnology.* 27 (2016) 75702. doi:10.1088/0957-4484/27/7/075702.
- [114] Y.Y. Chen, R. Walvekar, M. Khalid, K. Shahbaz, T.C.S.M. Gupta, Stability and thermophysical studies on deep eutectic solvent based carbon nanotube nanofluid Stability and thermophysical studies on deep eutectic solvent based carbon nanotube nanofluid, *Mater. Res. Express.* 4 (2017). doi:10.1088/2053-1591/aa77c7.
- [115] K. Pietrak, T.S. Wiśniewski, A review of models for effective thermal conductivity of composite materials, *J. Power Technol.* 95 (2014) 14–24.
- [116] H. Chen, Y. He, J. Zhu, H. Alias, Y. Ding, P. Nancarrow, C. Hardacre, D. Rooney, C. Tan, Rheological and heat transfer behaviour of the ionic liquid, [C4mim][NTf2], *Int. J. Heat Fluid Flow.* 29 (2008) 149–155.
- [117] P. Dehury, A.K. Upadhyay, T. Banerjee, Evaluation and conceptual design of triphenylphosphonium bromide-based deep eutectic solvent as novel thermal nanofluid for concentrated solar power, *Bull. Mater. Sci.* (2019). doi:10.1007/s12034-019-1946-6.
- [118] M. Osama, W. Rashmi, S. Kaveh, M. Khalid, T.C.S.M. Gupta, Theoretical modelling of thermal conductivity of deep eutectic solvent based nanofluid, *J. Eng. Sci. Technol.* 12 (2017) 809–819.
- [119] R. Walvekar, I.A. Faris, M. Khalid, Thermal conductivity of carbon nanotube nanofluid-experimental and theoretical study, *Heat Transf. Res.* 41 (2012) 145–163.
- [120] D.H. Kumar, H.E. Patel, V.R.R. Kumar, T. Sundararajan, T. Pradeep, S.K. Das, Model for heat conduction in nanofluids, *Phys. Rev. Lett.* 93 (2004) 144301.
- [121] C.T. Siong, R. Daik, M. Azmi, A. Hamid, C. Tze, R. Daik, M. Azmi, A. Hamid, Thermally Conductive of Nanofluid from Surfactant Doped Polyaniline Nanoparticle and Deep Eutectic Ionic



- [122] B. Wang, X. Wang, W. Lou, J. Hao, Gold-ionic liquid nanofluids with preferably tribological properties and thermal conductivity, *Nanoscale Res. Lett.* 6 (2011) 1–10.
- [123] G.H. Abdullah, N. Albayati, M. Kadhom, Investigating the Choline Chloride: Urea and Choline Chloride: Glycerol Deep Eutectic Solvents as Nanofluids Dispersants for Convective Heat Transfer, *Res. Rev. J. Eng. Sci. Technol.* 7 (2018) 64–73. <http://www.rroj.com/open-access/investigating-the-choline-chloride-urea-and-choline-chloride-glycerol-deep-eutectic-solvents-as-nanofluids-dispersants-forconvectiv.pdf>.
- [124] V. Gnielinski, New equations for heat and mass transfer in turbulent pipe and channel flow, *Int. Chem. Eng.* 16 (1976) 359–368.
- [125] W. Duangthongsuk, S. Wongwises, Heat transfer enhancement and pressure drop characteristics of TiO<sub>2</sub>–water nanofluid in a double-tube counter flow heat exchanger, *Int. J. Heat Mass Transf.* 52 (2009) 2059–2067.
- [126] J. Navas, A. Sánchez-coronilla, E.I. Martín, M. Toledo, J.J. Gallardo, T. Aguilar, R. Gómez-villarejo, R. Alcántara, C. Fernández-lorenzo, J.C. Pinero, J. Martín-Calleja, On the enhancement of heat transfer fluid for concentrating solar power using Cu and Ni nanofluids: An experimental and molecular dynamics study, *Nano Energy.* 27 (2016) 213–224. doi:10.1016/j.nanoen.2016.07.004.
- [127] R. Gomez-Villarego, P. Estelle, J. Navas, Boron nitride nanotubes-based nanofluids with enhanced thermal properties for use as heat transfer fluids in solar thermal applications, *Sol. Energy Mater. Sol. Cells.* 205 (2020) 110266. doi:10.1016/j.solmat.2019.110266.
- [128] J. Navas, P. Martinez-Merino, A. Sanchez-Coronilla, J.J. Gallardo, R. Alcantara, E.I. Martin, J.C. Pinero, J.R. Leon, T. Aguilar, J.H. Toledo, C. Fernandez-Lorenzo, MoS<sub>2</sub> nanosheets vs nanowires: preparation and theoretical study of highly stable and efficient nanofluids for Concentrating Solar Power, *J. Mater. Chem. A.* 6 (2018) 14919–14929. doi:10.1039/C8TA03817A.
- [129] K.R. Siongco, R.B. Leron, A.R. Caparanga, M. Li, Molar heat capacities and electrical conductivities of two ammonium-based deep eutectic solvents and their aqueous solutions, *Thermochim. Acta.* 566 (2013) 50–56. doi:10.1016/j.tca.2013.05.023.
- [130] F.S.G. Bagh, K. Shahbaz, F.S. Mjalli, I.M. Alnashef, M.A. Hashim, Fluid Phase Equilibria Electrical conductivity of ammonium and phosphonium based deep eutectic solvents : Measurements and artificial intelligence-based prediction, *Fluid Phase Equilib.* 356 (2013) 30–37.

- [131] A. Basaiahgari, S. Panda, R.L. Gardas, Acoustic, volumetric, transport, optical and rheological properties of Benzyltripropylammonium based Deep Eutectic Solvents, *Fluid Phase Equilib.* (2017) 3–11. doi:10.1016/j.fluid.2017.03.011.
- [132] M. Kuddushi, G.S. Nangala, S. Rajput, S.P. Ijardar, N.I. Malek, Understanding the peculiar effect of water on the physicochemical properties of choline chloride based deep eutectic solvents theoretically and experimentally, *J. Mol. Liq.* 278 (2019) 607–615. doi:10.1016/j.molliq.2019.01.053.
- [133] A. Singh, R. Walvekar, Mohammad Khalid, W.Y. Wong, T.C.S.M. Gupta, Thermophysical properties of glycerol and polyethylene glycol (PEG 600) based DES, *J. Mol. Liq.* 252 (2018) 439–444. doi:10.1016/j.molliq.2017.10.030.
- [134] R. Haghbakhsh, R. Bardool, A. Bakhtyari, A.R.C. Duarte, S. Raissi, Simple and global correlation for the densities of deep eutectic solvents, *J. Mol. Liq.* 296 (2019) 111830. doi:10.1016/j.molliq.2019.111830.
- [135] R. Alcalde, A. Gutiérrez, M. Atilhan, S. Aparicio, An experimental and theoretical investigation of the physicochemical properties on choline chloride – Lactic acid based natural deep eutectic solvent (NADES), *J. Mol. Liq.* 290 (2019) 110916. doi:10.1016/j.molliq.2019.110916.
- [136] P. Dehury, R.K. Chaudhary, T. Banerjee, A. Dalal, Evaluation of Thermophysical Properties of Menthol-Based Deep Eutectic Solvent as a Thermal Fluid : Forced Convection and Numerical Studies, *Ind. Eng. Chem. Res.* (2019). doi:10.1021/acs.iecr.9b01836.
- [137] H. Ghaedi, M. Ayoub, S. Suiher, S. Mekuria, G. Murshid, S. Nawaz, Thermal stability analysis, experimental conductivity and pH of phosphonium-based deep eutectic solvents and their prediction by a new empirical equation, *J. Chem. Thermodyn.* 116 (2018) 50–60. doi:10.1016/j.jct.2017.08.029.
- [138] A. Mohebbi, S. Baroutian, Estimation of particle concentration emitted from the stacks of Kerman Cement Plant using artificial neural networks, *Chem. Eng. Commun.* 195 (2008) 821–833.
- [139] G.H. Gu, J. Noh, I. Kim, Y. Jung, Machine learning for renewable energy materials, *J. Mater. Chem. A.* 7 (2019) 17096–17117.
- [140] Z.-M. Jiang, L.-J. Wang, Z. Gao, B. Zhuang, Q. Yin, E.-H. Liu, Green and efficient extraction of different types of bioactive alkaloids using deep eutectic solvents, *Microchem. J.* 145 (2019) 345–353.
- [141] K. Shahbaz, S. Baroutian, F.S. Mjalli, M.A. Hashim, I.M. AlNashef, Prediction of glycerol removal

intelligence techniques, *Chemom. Intell. Lab. Syst.* 118 (2012) 193–199.

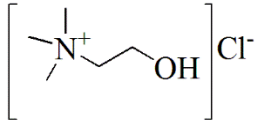
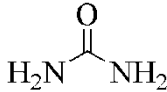
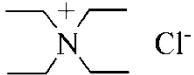
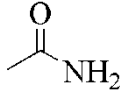
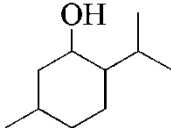
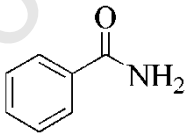
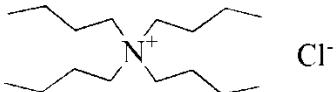
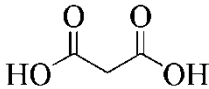
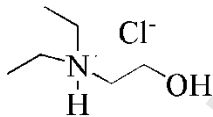
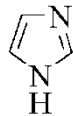
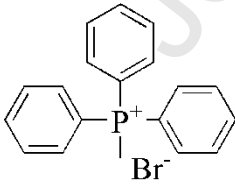
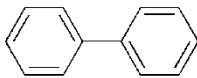
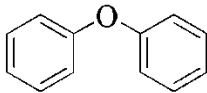
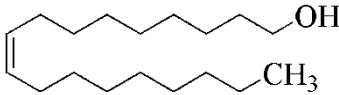
- [142] S.S. Fiyadh, M.A. AlSaadi, W.Z. Binti Jaafar, M.K. AlOmar, S.S. Fayaed, A.R. Hama, L.S. Hin, A. El-Shafie, Mercury removal from water using deep eutectic solvents-functionalized multi walled carbon nanotubes: Nonlinear autoregressive network with an exogenous input neural network approach, *Environ. Prog. Sustain. Energy.* 38 (2019) e13261.
- [143] S.S. Fiyadh, M.A. AlSaadi, M.K. AlOmar, S.S. Fayaed, A. El-Shafie, Lead removal from water using DES functionalized CNTs: ANN modeling approach, *Desalin. Water Treat.* 150 (2019) 105–113.
- [144] S.S. Fiyadh, M.A. AlSaadi, M.K. AlOmar, S.S. Fayaed, A.R. Hama, S. Bee, A. El-Shafie, The modelling of lead removal from water by deep eutectic solvents functionalized CNTs: artificial neural network (ANN) approach, *Water Sci. Technol.* 76 (2017) 2413–2426.
- [145] S.S. Fiyadh, M.A. AlSaadi, M.K. AlOmar, S.S. Fayaed, A. El-Shafie, Arsenic removal from water using N, N-diethylethanolammonium chloride based DES-functionalized CNTs:(NARX) neural network approach, *J. Water Supply Res. Technol.* (2018) 531–542.
- [146] S.S. Fiyadh, M.A. AlSaadi, M.K. AlOmar, S.S. Fayaed, F.S. Mjalli, A. El-Shafie, BTPC-Based DES-Functionalized CNTs for As<sup>3+</sup> Removal from Water: NARX Neural Network Approach, *J. Environ. Eng.* 144 (2018) 4018070.
- [147] I. Adeyemi, M.R.M. Abu-zahra, L.F. Vega, Physicochemical properties of alkanolamine-choline chloride deep eutectic solvents: Measurements, group contribution and artificial intelligence prediction techniques, *J. Mol. Liq.* 256 (2018) 581–590. doi:10.1016/j.molliq.2018.02.085.
- [148] A.Z. Hezave, M. Lashtabzadeh, S. Raeissi, Using artificial neural network to predict the ternary electrical conductivity of ionic liquid systems, *Fluid Phase Equilib.* 314 (2012) 128–133.
- [149] D. Bahamon, M.R.M. Abu-Zahra, L.F. Vega, Molecular simulations of carbon-based materials for selected CO<sub>2</sub> separation and water treatment processes, *Fluid Phase Equilib.* 492 (2019) 10–25.
- [150] H. Sun, Y. Li, X. Wu, G. Li, Theoretical study on the structures and properties of mixtures of urea and choline chloride, *J. Mol. Model.* 19 (2013) 2433–2441.
- [151] S.L. Perkins, P. Painter, C.M. Colina, Molecular dynamic simulations and vibrational analysis of an ionic liquid analogue, *J. Phys. Chem. B.* 117 (2013) 10250–10260.
- [152] M. Atilhan, S. Aparicio, Molecular Dynamics Simulations of Metal Nanoparticles in Deep Eutectic Solvents, *J. Phys. Chem. C.* 122 (2018) 18029–18039. doi:10.1021/acs.jpcc.8b02582.

microsecond time scale, *J. Chem. Theory Comput.* 5 (2009) 1632–1639.

[154] J.-H. Lee, S.-H. Lee, C. Choi, S. Jang, S. Choi, A review of thermal conductivity data, mechanisms and models for nanofluids, *Int. J. Micro-Nano Scale Transp.* (2011).

[155] I.I.I. Alkhatib, D. Bahamon, F. Llovel, M.R.M. Abu-Zahra, L.F. Vega, Perspectives and guidelines on thermodynamic modelling of deep eutectic solvents, *J. Mol. Liq.* 298 (2020) 112183. doi:10.1016/j.molliq.2019.112183.

[156] F.S. Mjalli, G. Murshid, S. Al-Zakwani, A. Hayyan, Monoethanolamine-based deep eutectic solvents, their synthesis and characterization, *Fluid Phase Equilib.* 448 (2017) 30–40. doi:10.1016/j.fluid.2017.03.008.

Hydrogen Bond Acceptor (HBA)	Hydrogen Bond Donor (HBD)
 <p>Choline Chloride (C<sub>5</sub>H<sub>14</sub>ClNO)</p>	 <p>Urea (CH<sub>4</sub>N<sub>2</sub>O)</p>
 <p>Tetraethylammonium Chloride (C<sub>8</sub>H<sub>20</sub>ClN)</p>	 <p>Acetamide (C<sub>2</sub>H<sub>5</sub>NO)</p>
 <p>DL-Menthol (C<sub>10</sub>H<sub>20</sub>O)</p>	 <p>Benzamide (C<sub>7</sub>H<sub>7</sub>NO)</p>
 <p>Tetrabutylammonium Chloride (C<sub>16</sub>H<sub>36</sub>ClN)</p>	 <p>Malonic Acid (C<sub>3</sub>H<sub>4</sub>O<sub>4</sub>)</p>
 <p>N,N-diethyl-2-hydroxy ethanamide dihydrochloride (C<sub>6</sub>H<sub>16</sub>Cl<sub>2</sub>N<sub>2</sub>O)</p>	 <p>Imidazole (C<sub>3</sub>H<sub>4</sub>N<sub>2</sub>)</p>
 <p>Methyltriphenylphosphonium bromide (C<sub>19</sub>H<sub>18</sub>BrP)</p>	 <p>Biphenyl (C<sub>12</sub>H<sub>10</sub>)</p>
 <p>Diphenyl Ether (C<sub>12</sub>H<sub>10</sub>O)</p>	 <p>Oleyl Alcohol (C<sub>18</sub>H<sub>36</sub>O)</p>

#	HBA	HBD	Molar ratio	Ref
1	Choline chloride	Glycerol	1:2	[64,74]
2	Choline chloride	Urea	1:2	[75,76]
3	Choline chloride	Ethylene glycol	1:2	[33,76,77]
4	Choline chloride	Acetic acid	1:2	[76]
5	Choline chloride	Caffeic acid	1:0.5	[78,79]
6	Choline chloride	1,2-butanediol	1:2	[80]
7	Betaine	Urea	1:2	[76,81]
8	Betaine	Ethylene glycol	1:1	[81]
9	Betaine	Glycerol	1:2	[81]
10	Betaine	Sorbitol	3:1	[65]
11	Choline chloride	Ethylene glycol	1:1.78	[66]
12	Choline chloride	Ethylene glycol	1:2.03	[66]
13	Choline chloride	Ethylene glycol	1:2.57	[66]
14	Choline chloride	Glycolic acid	1:1	[67]
15	Choline chloride	Glycerol	1:1	[66]
16	Choline chloride	Glycerol	1:2.03	[66]
17	Choline chloride	Glycerol	1:3	[66]
18	Methyl triphenylphosphonium bromide	Ethylene glycol	1:3	[66]
19	Methyl triphenylphosphonium bromide	Ethylene glycol	1:4	[66,68]
20	Methyl triphenylphosphonium bromide	Ethylene glycol	1:5.25	[66]
21	Methyl triphenylphosphonium bromide	Glycerol	1:1.75	[68]
22	L-proline	Lactic acid	1:1	[69]
23	L-proline	Malvulinic acid	1:2	[69]
24	Diethylamine hydrochloride	Guaiacol	1:3	[71]
25	Diethylamine hydrochloride	Guaiacol	1:4	[71]
26	Diethylamine hydrochloride	Guaiacol	1:5	[71]
27	Trimethylglycine	2-Chloro benzoic acid	1:2	[70]
28	Trimethylglycine	Benzoic acid	1:2	[70]
29	Trimethylglycine	Phenylacetic acid	1:2	[70]
30	Trimethylglycine	Mandelic acid	1:2	[70]
31	Tetrabutylammonium chloride	Glycerol	1:3	[72]
32	Tetrabutylammonium chloride	Glycerol	1:4	[72]
33	Tetrabutylammonium chloride	Glycerol	1:5	[72]
34	Tetrabutylammonium chloride	Ethylene glycol	1:2	[72]
35	Tetrabutylammonium chloride	Ethylene glycol	1:3	[72]
36	Tetrabutylammonium chloride	Ethylene glycol	1:4	[72]
37	Tetrabutylammonium chloride	Triethylene glycol	1:1	[72]
38	Tetrabutylammonium chloride	Triethylene glycol	2:1	[72]
39	Tetrabutylammonium chloride	Triethylene glycol	3:1	[72]
40	Tetrabutylammonium chloride	Triethylene glycol	4:1	[72]
41	N,N diethylenethanol ammonium chloride	Glycerol	1:2.03	[66]
42	N,N diethylenethanol ammonium chloride	Glycerol	1:3	[66]
43	N,N diethylenethanol ammonium chloride	Glycerol	1:4	[66]
44	N,N diethylenethanol ammonium chloride	Ethylene glycol	1:2.03	[66]
45	N,N diethylenethanol ammonium chloride	Ethylene glycol	1:3	[66]
46	N,N diethylenethanol ammonium chloride	Ethylene glycol	1:4	[66]
47	Acetyl choline chloride	Imidazole	1:1.5	[73]
48	Acetyl choline chloride	Imidazole	1:2	[73]
49	Acetyl choline chloride	Imidazole	1:3	[73]
50	Acetyl choline chloride	1,2,4-triazole	1:1	[73]

**Table 3.** Summary of some studies on characterization of deep eutectic solvents (DESs).

Author	DES (molar ratio)	TC* ( $\text{Wm}^{-1}\text{K}^{-1}$ )	Viscosity (mPa.s)	Density ( $\text{kg.m}^{-3}$ )	Other
Lapeña et al. [104]	Choline chloride + Ethylene glycol (1:2)	-	100.9-10.90 (278.15-338.15K)	1127.50-1093.32 (278.15-338.15K)	$\kappa_s, n_D, C_{pm}, u, \sigma, \kappa, \nu$
	ChCl + EG + Water (1:1.98:0.95)	-	66.65-7.966 (278.15-338.15K)	1123.47-1089.54 (278.15-338.15K)	
	ChCl + Monoethanol amine (1:5)	-	48.4642-6.1433 (298-358K)	1076.8-1035.0 (298-358K)	
	ChCl + Monoethanol amine (1:6)	-	36.6894-5.4608 (298-358K)	1069.2-1025.2 (298-358K)	
	ChCl + Monoethanol amine (1:7)	-	37.7133-5.2901 (298-358K)	1065.0-1020.8 (298-358K)	
	ChCl + Monoethanol amine (1:8)	-	32.5939-4.4369 (298-358K)	1062.8-1018.0 (298-358K)	
	MTPB + Monoethanol amine (1:5)	-	131.4744-9.4231 (298-358K)	1195.4-1149.3 (298-358K)	
Mjalli et al. [156]	MTPB + Monoethanol amine (1:6)	-	34.5513-5.2335 (298-358K)	1107.7-1059.9 (298-358K)	$n_D, \sigma$
	MTPB + Monoethanol amine (1:7)	-	28.2692-4.9359 (298-358K)	1099.7-1051.3 (298-358K)	
	MTPB + Monoethanol amine (1:8)	-	27.2718-4.4872 (298-358K)	1093.5-1045.1 (298-358K)	
	TBAB + Monoethanol amine (1:3)	-	107.0784-11.0000 (298-358K)	1062.0-1019.1 (298-358K)	
	TBAB + Monoethanol amine (1:4)	-	80.4117-8.6470 (298-358K)	1061.1-1017.4 (298-358K)	
	TBAB + Monoethanol amine (1:5)	-	52.9616-5.9019 (298-358K)	1056.6-1012.0 (298-358K)	
	TBAB + Monoethanol amine (1:6)	-	22.3725-5.9019 (298-358K)	1048.0-991.7 (298-358K)	
	Choline chloride + Urea (1:2)	0.245-0.231 (298-343K)	-	-	
Gautam et al. [99]	NDAC + Urea (1:2)	0.242-0.230 (298-343K)	-	-	$u$
	Choline chloride + Thiourea (1:2)	0.182-0.170 (298-343K)	1122-333 (288.15-333.15K)	-	
Lapeña et al. [107]	Choline chloride + Urea (1:2)	-	5966-76.13 (288.15-338.15K)	1205.14-1178.13 (288.15-338.15K)	$\kappa_s, n_D, C_{pm}, u, \sigma, \kappa, \nu$
	Choline chloride + Urea + Water	-	139.8-9.86 (278.15-338.15K)	1185.88-1153.78 (278.15-338.15K)	
Zhu et al. [106]	Choline chloride + Phenol (1:2)	-	137.73-19.5 (293.15-333.15K)	1098.7-1065.3 (293.15-333.15K)	$n_D$
	Choline chloride + P-cresol (1:2)	-	133.68-19.6 (293.15-333.15K)	1071.9-1039.7 (293.15-333.15K)	
	Choline chloride + P-chlorophenol (1:2)	-	170.64-23.5 (293.15-333.15K)	1203.1-1167.9 (293.15-333.15K)	
Hong-Zhen et al. [105]	TBAC + Propionic acid (1:2)	-	300.3155-26.498 (288-338K)	972.1-939.5 (288-338K)	$\kappa, n_D$
	TBAC + Ethylene glycol (1:2)	-	216.4038-19.874 (288-338K)	995.1-964.5 (288-338K)	

Sedghamiz et al. [109]	TBAC + Polyethylene glycol (1:2)	-	313.5647-30.915 (288-338K)	1084.1-1048.5 (288-338K)	$\kappa$ , $n_D$
	TBAC + Phenylacetic acid (1:2)	-	675.7098-30.915 (288-338K)	1046.6-1014.5 (288-338K)	
	NaCl + Ethylene glycol (0.5:2)	-	32.360-7.348 (293.15-333.15K)	1148.8-1121.5 (293.15-333.15K)	
	NaBr + Ethylene glycol (0.5:1)	-	64.464-12.287 (293.15-333.15K)	1306.8-1277.9 (293.15-333.15K)	
	NaI + Ethylene glycol (0.5:1)	-	81.232-14.158 (293.15-333.15K)	1497.1-1464.8 (293.15-333.15K)	
	L-proline + levulinic acid (1:2)	-	955.0-73.4 (303.15-343.15K)	1201-1164 (293.15-343.15K)	
Sánchez et al. [69]	L-proline + DL-lactic acid (1:1)	-	997.4-246.1 (323.15-343.15K)	1265-1230 (293.15-343.15K)	$u$ , $n_D$ , $\kappa_s$
	Betaine + DL-lactic acid (1:2)	-	1266.0-65.9 (298.15-343.15K)	1201-1169 (298.15-343.15K)	
	Betaine + DL-lactic acid (1:5)	-	386.6-20.6 (293.15-343.15K)	1209-1169 (293.15-343.15K)	
	Betaine + levulinic acid (1:2)	-	1342-67.0 (298.15-343.15K)	1162-1126 (293.15-343.15K)	
	Betaine + DL-lactic acid + Water (1:1:1)	-	690.4-37.9 (293.15-343.15K)	1184-1152 (293.15-343.15K)	
	Betaine + Citric acid + Water (2:1:6)	-	1057.0-90.0 (303.15-343.15K)	1263-1231 (293.15-343.15K)	
Singh et al. [133]	Choline chloride + Glycerol (1:2)	-30.66_-23.58 %E.(298-368K)	195.1-18.6 (298-373K)	1187.8-1151.5 (298-363K)	-
	Choline chloride + Glycerol (1:3)	-26.52_-19.75 %E.(298-368K)	247.8-18.4 (298-373K)	1203.6-1166.5 (298-363K)	
	Choline chloride + Glycerol (1:4)	-17.83_-11.26 %E.(298-368K)	238.5-18.6 (298-373K)	1208.8-1171.2 (298-363K)	
	Choline chloride + Glycerol (1:5)	-17.42_-14.29 %E.(298-363K)	297.3-18.5 (298-373K)	1215.6-1176.7 (298-363K)	
	Polyethylene glycol + Glycerol (1:3:2)	1.35_-26.09 %F (298-363K)	194.9-14.7 (298-373K)	1133.9-1082.3 (298-363K)	
	Polyethylene glycol + Glycerol (1:4:2)	0.96_-25.87 %E (293-368K)	182.4-16.8 (298-373K)	1135.2-1083.6 (298-363K)	
	Polyethylene glycol + Glycerol (1:5:2)	1.35_-16.82 %E.(298-368K)	168.5-14.7 (298-373K)	1131.7-1080.2 (298-363K)	
	Betaine + EG + Lactic acid (1:1:1)	-	144.6-12.8 (303-363K)	1215-1183 (298-348K)	
	Alanine + LA + Citric acid (1:3:1)	-	453.5-77.9 (333-363K)	1332-1331 (298-348K)	
	Choline chloride + EG + LA (1:2:1)	-	28.7-4.9 (303-363K)	1184-1153 (298-348K)	
Škulcová et al. [108]	Betaine + Glycerol + Citric acid (1:2:1)	-	468.5-158.2 (343-363K)	1249-1242 (298-348K)	-
	Proline + LA+ Citric acid (1:3:1)	-	375.5-71.4 (333-363K)	1225-1223 (298-348K)	
	Proline + Glycerol + Citric acid (1:4:1)	-	318.5-69.2 (333-363K)	1304-1272 (298-348K)	
	Malic acid + Proline + LA (1:2:4)	-	590.6-58.4 (323-363K)	1292-1266 (298-348K)	
	Malic acid + Alanine + LA (1:1:3)	-	291.2-56.5 (333-363K)	1310-1275 (298-348K)	
	Betaine + Propanediol + LA (1:3:1)	-	115.0-8.9 (303-363K)	1118-1087 (298-348K)	



	Betaine + Urea + Glycerol (1:2:3)	-	301.9-22.3 (313-363K)	1284-1255 (298-348K)	
	Malonic acid+ChCl+Propanediol (1:1:3)	-	84.0-9.9 (303-363K)	1187-1118 (298-348K)	
Siongco et al. [110]	NDAC + Glycerol (1:2)	-	513.09-42.57 (298.15-343.15K)	1176.6-1149.2 (298.15-343K)	$n_D$
	NDAC + Ethylene glycol (1:2)	-	50.44-9.986 (298.15-343.15K)	1099.9-1072.8 (298.15-343K)	
	BTAC + Phenol (1:3)	-	647.303-24.896 (293-343K)	1060.26-1027.57 (293-343K)	
Basaiahgari et al. [131]	BTAC + Ethylene glycol 1:3)	-	340.25-24.896 (293-343K)	1063.45-1032.75 (293-343K)	$u, n_D, V_m, R_m, F_m$
	BTAC + Lactic acid (1:3)	-	2282.16-82.9876 (303-343K)	1120.86-1084.98 (293-343K)	
	BTAC + Glycerol (1:3)	-	1883.82-99.5851 (303-343K)	1.13322-1.10212 (293-343K)	
	TBAC + Glycerol (1:3)	-	1170.23-36.24 (293.15-353.15K)	1105.2-1067.0 (293.15-353.15K)	
	TBAC + Glycerol (1:4)	-	952.75-36.25 (293.15-353.15K)	1130.1-1090.9 (293.15-353.15K)	
	TBAC + Glycerol (1:5)	-	1102.91-36.23 (293.15-353.15K)	1145.4-1106.2 (293.15-353.15K)	
	TBAC + Ethylene glycol (1:2)	-	211.94-17.50 (293.15-353.15K)	1014.1-975.5 (293.15-353.15K)	
Mjalli et al. [72]	TBAC + Ethylene glycol (1:3)	-	103.67-11.25 (293.15-353.15K)	1029.1-990.9 (293.15-353.15K)	$\sigma, \kappa, n_D, pH$
	TBAC + Ethylene glycol (1:4)	-	85.64-11.25 (293.15-353.15K)	1040.3-999.9 (293.15-353.15K)	
	TBAC + Triethylene glycol (1:1)	-	863.16-42.10 (293.15-353.15K)	1027.1-990.9 (293.15-353.15K)	
	TBAC + Triethylene glycol (2:1)	-	1410.52-105.26 (303.15-353.15K)	1007.1-970.0 (293.15-353.15K)	
	TBAC + Triethylene glycol (3:1)	-	7031.58-63.16 (313.15-353.15K)	996.3-960.3 (293.15-353.15K)	
	TBAC + Triethylene glycol (4:1)	-	3263.16-84.21 (303.15-353.15K)	990.0-954.9 (293.15-353.15K)	

TC: Thermal conductivity, Other: Other reported thermophysical properties, EG: Ethylene glycol, ChCl: Choline chloride, MTPB: Methyl triphynole phosphonium bromide, TBAB: Tetrabutyl ammonium bromide, TBAC: Tetrabutyl ammonium chloride. NDAC: N,N-diethylethanol ammonium chloride, BTAC: Benzyl tripropyl ammonium chloride, LA: Lactic acid. %E.: Enhancement percentage of thermal conductivity.  $n_D$ : Refractive index, Cpm: Isobaric molar heat capacity,  $\sigma$ : Surface tension,  $u$ : speed of sound,  $\kappa$ : Electrical conductivity,  $\kappa_s$ : Isentropic compressibility,  $\nu$ : Kinematic viscosity,  $V_m$ : Molar volume,  $R_m$ : Molar refractivity, and  $F_m$ : Free volume.

**Table 4.** Summary of case studies of using DES as base fluid.

Author	Nanoparticle	DES	Stability	Studied properties	Working T (K)	Instrument	Np Con.	Comments	Ref
Fang et al.	Graphene oxide	Choline chloride + Ethylene glycol	~4 weeks	Thermal conductivity Specific heat capacity	298, 303	KD2 Pro Thermal properties analyzer	0.01	<ul style="list-style-type: none"> <li>• Increment in HBD amount, and decrement in graphene oxide concentration leads to enhancing stability.</li> <li>• 85% increase in TC for nanofluids based on ChCl:TEG (1:3) with rising T from 298 to 343K.</li> <li>• 177% increase in TC for nanofluids based on MTPB:TEG (1:5) with rising T from 298 to 343K.</li> </ul>	[113]
		Choline chloride + Triethylene glycol			313, 323		0.02		
		Methyl-triphenyl phosphonium bromide + EG Methyl-triphenyl phosphonium bromide +TEG			333, 343		0.03 (wt%)		
Chen et al.	MWCNT (20nm×30µm)	Methyl-triphenyl phosphonium-bromide + EG	3 day	Thermal Conductivity	298	KI 2 Pro	0.01	<ul style="list-style-type: none"> <li>• TC was enhanced by increasing temperature and concentration of CNT.</li> <li>• Max thermal enhancement for NFs based on EG with 1:5 ChCl, at 0.08 wt% and 323K was 24.4%.</li> <li>• Min thermal enhancement for NFs based on EG with 1:3 ChCl, at 0.01 wt% and 298K was 0.1%.</li> <li>• Nanofluids based on TEG were not indicated any significant thermal improvement.</li> </ul>	[114]
		Methyl-triphenyl phosphonium-bromide + TEG	4 day	Density	313	Anton Paar Density Meter	0.04		
		Choline chloride + Ethylene glycol	1 day	Viscosity	323	Rheometer	0.08		
		Choline chloride + Triethylene glycol	3 day	Specific heat capacity		Differential Scanning Calorimeter	(wt%)		
Dehury et al.	Alumina (50 nm) Spherical	Oleic acid + DL-Menthol	Few hours	Thermal conductivity	298 to 373	KD2 Pro Anton Paar density meter Anton Paar interfacial rheometer Differential Scanning Calorimeter Delsa Nano	0.001	<ul style="list-style-type: none"> <li>• 10% increase in thermal conductivity of nanofluids compared to DES.</li> <li>• Density decreased with rising in temperature.</li> <li>• DES and DES-based nanofluids had Newtonian behavior.</li> <li>• Heat capacity of nanofluids was enhanced by 6% at 0.001 and 50% at 0.01 v% compared to DES.</li> <li>• 0.005 was optimum volume fraction of alumina to represent more efficiency of thermal properties.</li> </ul>	[100]
				Density			0.005		
				Viscosity			0.0075		
				Specific heat capacity Zeta potential			0.01 (v%)		
Liu et al.	SiO <sub>2</sub> -SH SiO <sub>2</sub> -SH-DP SiO <sub>2</sub> -SH-DP-Cu	Choline chloride + Glycerol Choline chloride + Ethylene glycol	15 days	Thermal conductivity	303, 308	Xiotech Liquid TC analyzer Digital rotary viscometer	1	<ul style="list-style-type: none"> <li>• 12.5% increase in thermal conductivity for glycerol:ChCl.</li> <li>• 13.6% increase in thermal conductivity for EG:ChCl based nanofluids.</li> <li>• Viscosity decreased until a mass fraction of 2.0% and then increases for higher content.</li> </ul>	[96]
				Thermal conductivity	313, 318		2		
				Viscosity	323, 328		3		
				Viscosity	323, 328		4		
				Viscosity	333, 338		5 (wt%)		
Dehury et al.	Alumina (50 nm)	Triphenylphosphonium bromide + EG	NA	Thermal conductivity	293, 298	KD2 Pro Anton Paar densitometer Anton Paar interfacial rheometer Differential Scanning Calorimeter	1	<ul style="list-style-type: none"> <li>• TC of DES and DES-based nanofluid increased by 70% compared to VP-1 and Downterm-A.</li> <li>• Viscosity and density decreased with rising in temperature.</li> </ul>	[117]
				Density	303, 308		(wt%)		
				Viscosity	313, 318				
				Specific heat capacity	323, 328				

				333			
Osama et al.	Graphene oxide	Methyl-triphenyl phosphonium bromide + EG	NA	Thermal conductivity	298	NA	0.01
					343		(wt%)
Siong et al.	DBSA-PANI (50-60 nm)	Choline Chloride + Urea	NA	Thermal conductivity	303	KD2 Pro	0.02
					313		
					323		0.05
							0.2
							0.4
							0.6
							0.8
							1.0
							(wt%)
Abdulla et al.	Al <sub>2</sub> O <sub>3</sub>	Choline chloride + Urea Choline chloride + Glycerol	NA	-	303- 43	-	1
							2
							3
							4
							5
							(wt%)
Liu et al.	TiO <sub>2</sub> (20 nm) Al <sub>2</sub> O <sub>3</sub> (30 nm) Graphene oxide	Choline chloride + Glycerol	1 week	Thermal conductivity	305, 310	Xiatech Liquid TC analyzer	0.2
				Viscosity	315, 320	Digital rotary viscometer	0.4
				Specific heat capacity	325, 330	Differential Scanning Calorimeter	0.8
				Zeta potential	335	Zetasizer Nano ZS analyzer	1.6
							(v%)

- There was not a specific pattern for TC enhancement versus increment of volume fraction.
- Data analyzed theoretically with two models based on Brownian motion, Rashmi's and Kumar's models. [118]
- Kumar's modified model developed to predict the thermal conductivity of DES-based nanofluids.
- With rising temperature, nanofluids based on DES with water showed higher improvement in TC than pure DES-based.
- TC enhancement of nanofluids attributed to Brownian motion and micro-convection of base fluids along with the interaction between dopants and DES ions. [121]
- Viscosity assessed as a function of temperature (303-343K) using modified Einstein's formula.
- ChCl:urea due to the possibility of institution self-hydrogen bonds between the urea and chloride ions represented higher viscosity than ChCl:glycerol.
- Existence of urea in DES molecular structure led to rising viscosity. [123]
- ChCl:urea had a higher friction factor than ChCl:glycerol.
- Pure DESs had higher heat transfer coefficient in comparison to their nanofluids.
- Thermal conductivity of developed nanofluids increased by from 3% to around 11.4%.
- Due to two-dimensional structure, graphene oxide displayed the least viscosity.
- By varying v.% of alumina, nanofluids exhibited a unique behavior of thermal conductivity, which FT-IR and <sup>1</sup>H NMR indicated hydrogen bond between glycerol and Al<sub>2</sub>O<sub>3</sub> was responsible for this unique phenomenon. [85]

**Table 5.** Summary of some theoretical studies on deep eutectic solvents (DESs).

Author	Deep eutectic solvent	Modeling method	Main object of study	Notes
Fiyadh et al. [145]	Glycerol + N,N-diethyl ethanol ammonium chloride	NARX neural network	Use of DES-functionalized CNTs as an adsorbent for arsenic removal from water	<ul style="list-style-type: none"> <li>- Input layer: time, adsorbent dosage, pH and initial concentration.</li> <li>- Optimum hidden layer: two hidden layers with 10 neurons in each one.</li> <li>- Output layer: adsorption capacity</li> <li>- Dataset: 156 data (training set: 136, test set: 20)</li> <li>- Training algorithm: back-propagation (trainlm)</li> <li>- Transfer function: tangent sigmoid (tansig)</li> <li>- Evaluators of model performance: RRMSE, MSE, RMSE, MAPE and RE.</li> </ul>
Fiyadh et al. [144]	Choline chloride + Triethylene glycol	feed-forward back-propagation (FFBP) neural network and layer recurrent (LR)	Usage of synthesized DES as functionalized agent with CNTs to adsorb ions of Pb <sup>2+</sup>	<ul style="list-style-type: none"> <li>- Input layer: pH, adsorbent dosage, contact time, and Pb<sup>2+</sup> initial concentration.</li> <li>- Hidden layer: 3 with 10 neurons (for FFBP), 5 with 10 neurons (for LR)</li> <li>- Output layer: adsorbent capacity of Pb<sup>2+</sup></li> <li>- Dataset: 158 runs</li> <li>- Evaluators for model performance: RMSE, RE, MSE, RRMSE and MAPE.</li> </ul>
Jiang et al. [140]	75 different types of synthesized DESs	Response surface methodology and Artificial neural network hybridized with genetic algorithm (GA)	Evaluation of efficiency of DESs on the extraction of Morphinane, Protoberberine, Bisbenzylisoquinoline, Indole and Quinolizidine alkaloids from five herbal medicines	<ul style="list-style-type: none"> <li>- Box-Behnken design was used to model extraction efficiency with 4 variables: water content, temperature, ultrasonic time and solid-liquid ratio at 3 levels.</li> <li>- Quality criterion of ANN: MSE and R<sup>2</sup></li> <li>- The most critical parameter for alkaloids extraction was water content in DESs.</li> </ul>
Fiyadh et al. [146]	Glycerol + Benzyl triphenyl phosphonium chloride	NARX neural network	Utilization of a DES as a functionalization agent of CNTs for arsenic ion removal from water	<ul style="list-style-type: none"> <li>- Pseudo-second order model was the best to describe adsorption kinetics.</li> <li>- Input layer: time, adsorbent dosage, pH, and initial concentration.</li> <li>- Hidden layer: two hidden layers with eight neurons in each one.</li> <li>- Output layer: adsorption capacity.</li> <li>- Training algorithm: Back-propagation (trainbr)</li> <li>- Transfer function: tangent sigmoid (tansig)</li> <li>- Evaluators of model performance: RRMSE, MSE, RMSE, MAPE, and RE.</li> </ul>
Shahbaz et al. [141]	9 DESs based on ammonium salt and 9 DESs based on phosphonium salt	feed-forward back-propagation neural network	Design a new modeling approach to predict glycerol removal by means of DESs	<ul style="list-style-type: none"> <li>- Input layer: DESs composition, mole fractions of DESs to biodiesel.</li> <li>- Hidden layer: 4 hidden neurons</li> <li>- Training algorithm: Levenberg–Marquardt optimization method</li> </ul>

Fiyadh et al. [142]	Glycerol + Tetra-n-butyl ammonium bromide	NARX neural network	Experimental and modeling process for Hg <sup>2+</sup> removal from water using functionalized MWCNT	<ul style="list-style-type: none"> <li>- Evaluators to model performance: IA, FB, NMSE, VG, MG, and R<sup>2</sup>.</li> <li>- Pseudo second order model was the best to describe kinetic mechanism.</li> <li>- Dataset: 163 data (training set: 143, test set: 20)</li> <li>- Input layer: Hg<sup>2+</sup> concentration, pH, amount of adsorbent dosage, and contact time.</li> <li>- Hidden layer: 2 with 10 neurons in each one.</li> <li>- Output layer: adsorbent's adsorption capacity.</li> <li>- Training algorithm: back-propagation (trainbr)</li> <li>- Transfer function: tangent sigmoid (tansig)</li> <li>- Evaluator for model performance: MSE, RMSE, RRMSE, MAPE, RE, and R<sup>2</sup>.</li> <li>- Density of DESs were predicted with three different methods.</li> <li>- Conductivity of DESs predicted with conventional ANN and bagging ANN.</li> </ul>
Adeyemi et al. [147]	Choline chloride + Monoethanolamine Choline chloride + Diethanolamine, Choline chloride + Methyl-diethanolamine	Empirical group contribution method Conventional ANN Bagging ANN	Measurements of conductivity, pH, density, viscosity, surface tension, and thermal stability of DESs experimentally	<ul style="list-style-type: none"> <li>- Deviations for group contribution and ANNs are high when compared to experimental values, due to the special nature of bonds.</li> <li>- Dataset: 105 data points (55% used for training).</li> <li>- Input layer: mole fraction of DES components, temperature, and molecular weight of DESs.</li> <li>- Bagging ANN provided the best model for density and conductivity.</li> </ul>
Kumar et al. [120]	-	Empirical models	Proposition of a model for TC enhancement of nanofluids and its temperature dependence	<ul style="list-style-type: none"> <li>- Developed model (Kumar's model) explained TC enhancement of nanofluid with respect to variation in particle size, particle volume fraction, and temperature.</li> <li>- For large concentration of nanoparticles which interparticle interactions become important, model may not be used.</li> </ul>
Walvekar et al. [119]	-	Empirical models	Study of TC of CNT-based nanofluid experimentally and theoretically	<ul style="list-style-type: none"> <li>- Rashmi's model was presented which demonstrated effect of diameter and aspect ratio of the CNTs and considered influence of temperature on TC enhancement.</li> <li>- Experimental TC values of DES-based nanofluids were compared with predicted TC values obtained two Brownian based models, Rashmi's and Kumar's models.</li> </ul>
Osama et al. [118]	Ethylene glycol + Methyl triphenyl phosphonium bromide	Empirical models	Analysis of thermal conductivity of graphene oxide nanoparticles dispersed in DESs	<ul style="list-style-type: none"> <li>- Evaluator of models' prediction quality: percentage deviation from the actual behavior</li> <li>- Kumar's modified model was made to improve predictions capability of</li> </ul>

Perkins et al. [151]	Choline chloride + Urea	Molecular dynamics simulation	Performing molecular dynamics simulations over a temperature range on a DES, using different force field modifications	<p>previous models.</p> <ul style="list-style-type: none"> <li>-Simulation boxes minimized by steepest descent method for 10 cycles, and conjugate gradient method used for 10000 cycles.</li> <li>-Temperature control: Langevin dynamics thermostat with a collision frequency of <math>5 \text{ ps}^{-1}</math>.</li> <li>-Key interactions between the moieties in DES interrupted the main interactions within parent substances and were responsible for the decrease in freezing point.</li> <li>-It was confirmed DESs acting as metal nanoparticle stabilizers.</li> </ul>
Atilhan et al. [152]	Choline chloride + Urea Choline chloride + Glycerol Choline chloride + Malonic acid Choline chloride + Levulinic acid Choline chloride + Ethylene glycol Choline chloride + Phenyl acetic acid	Molecular dynamics simulation	Analyzing mechanism of nanoparticles solvation and aggregation in DESs as a function of shape, size, type of nanoparticles, and HBDs	<ul style="list-style-type: none"> <li>-Temperature control: Langevin type thermostat, with <math>0.1 \text{ ps}^{-1}</math> damping constant.</li> <li>-Metal atoms (Au, Pt, Ag, Pd, Ni) were described as non-charged 12-6 Lennard-Jones sites.</li> <li>-Analysis of shape effect on solvation was indicated spherical nanoparticles led a slightly more efficient solvation in comparison with icosahedral ones.</li> <li>-With increment of urea concentration, hydrogen bond interactions between choline cations and <math>\text{Cl}^-</math> anions reduced.</li> <li>-From hydrogen bond lifetimes was shown 1:2 molar ration of choline chloride and urea is required for a valid strength of hydrogen interaction to keep low melting point of DES.</li> </ul>
Sun et al. [150]	Choline chloride + Urea	Molecular dynamics simulation	Performing molecular dynamic simulations to investigate the structures of DES and explanation of its low melting point	

NARX is nonlinear autoregressive network with exogenous input, neural network. RRMSE is relative root mean square error, MSE is mean square error, RMSE and MAPE are root mean square error and mean absolute percentage error, respectively and RE is relative error. IA is Index of Agreement. FB is Fractional Bias. NMSE, VG, and MG are normalized mean square error, geometric variance, and geometric mean bias respectively.

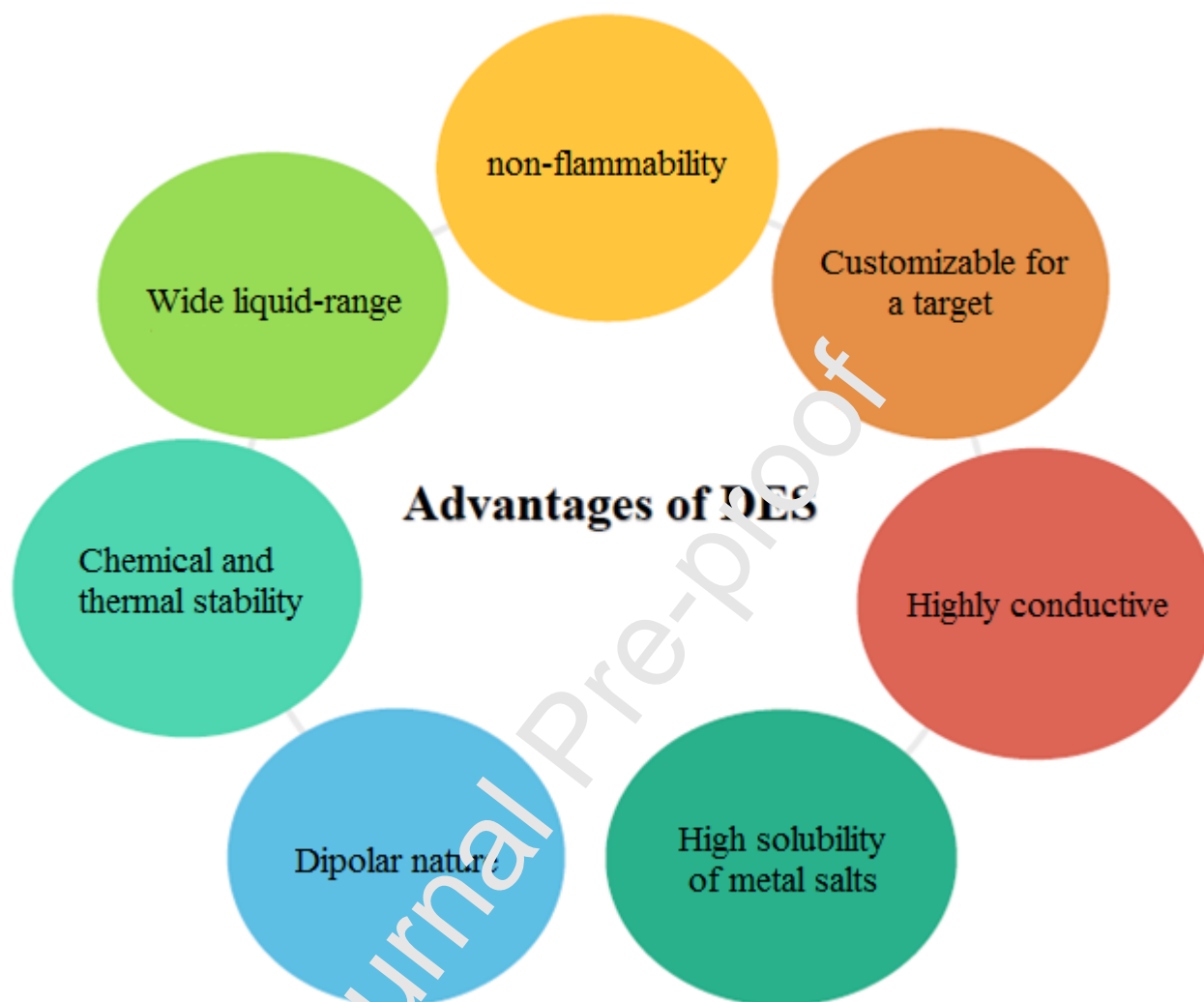


**Fig. 1.** Some prominent advantages of deep eutectic solvents.

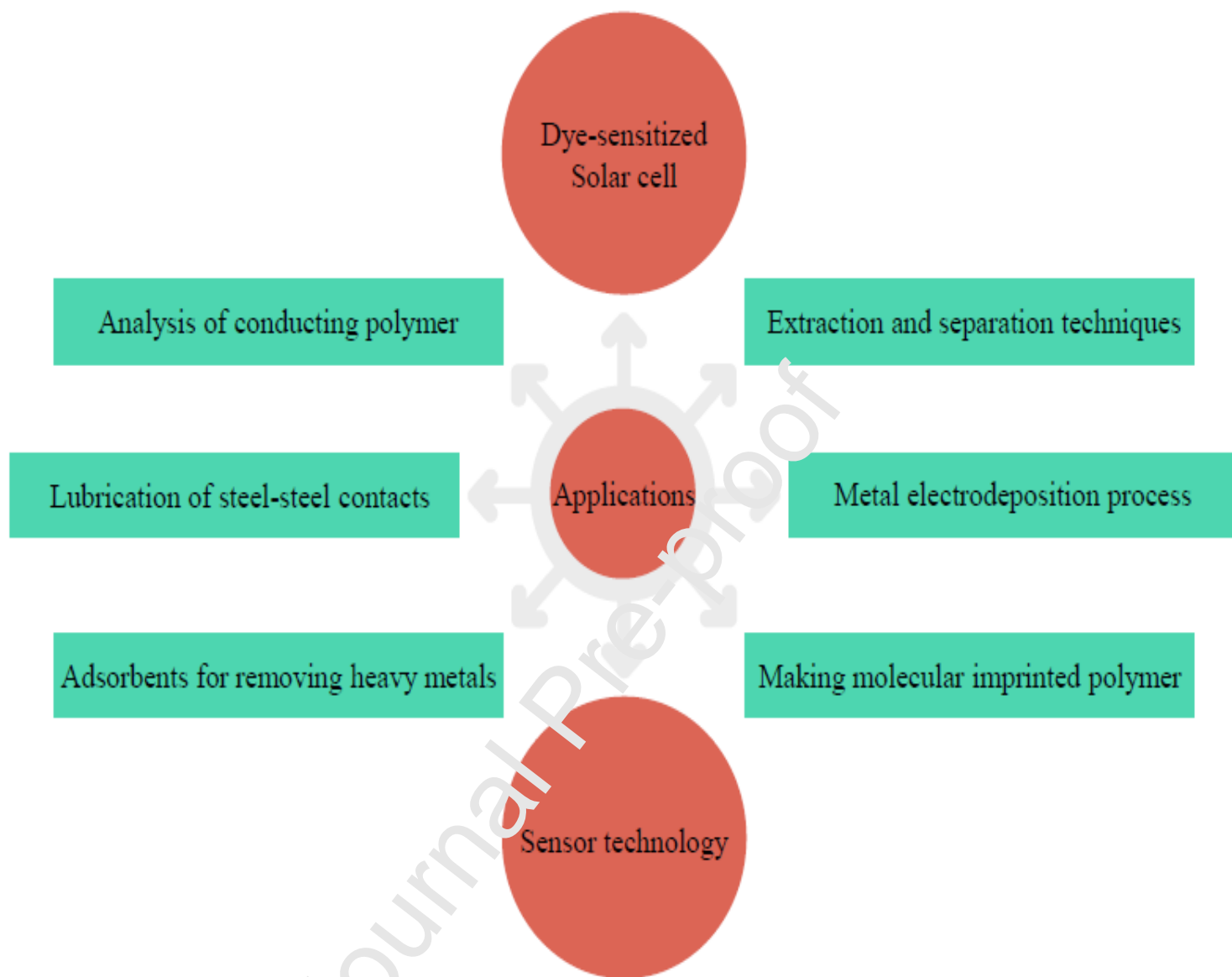


**Fig. 2.** Some notable applications of deep eutectic solvents.



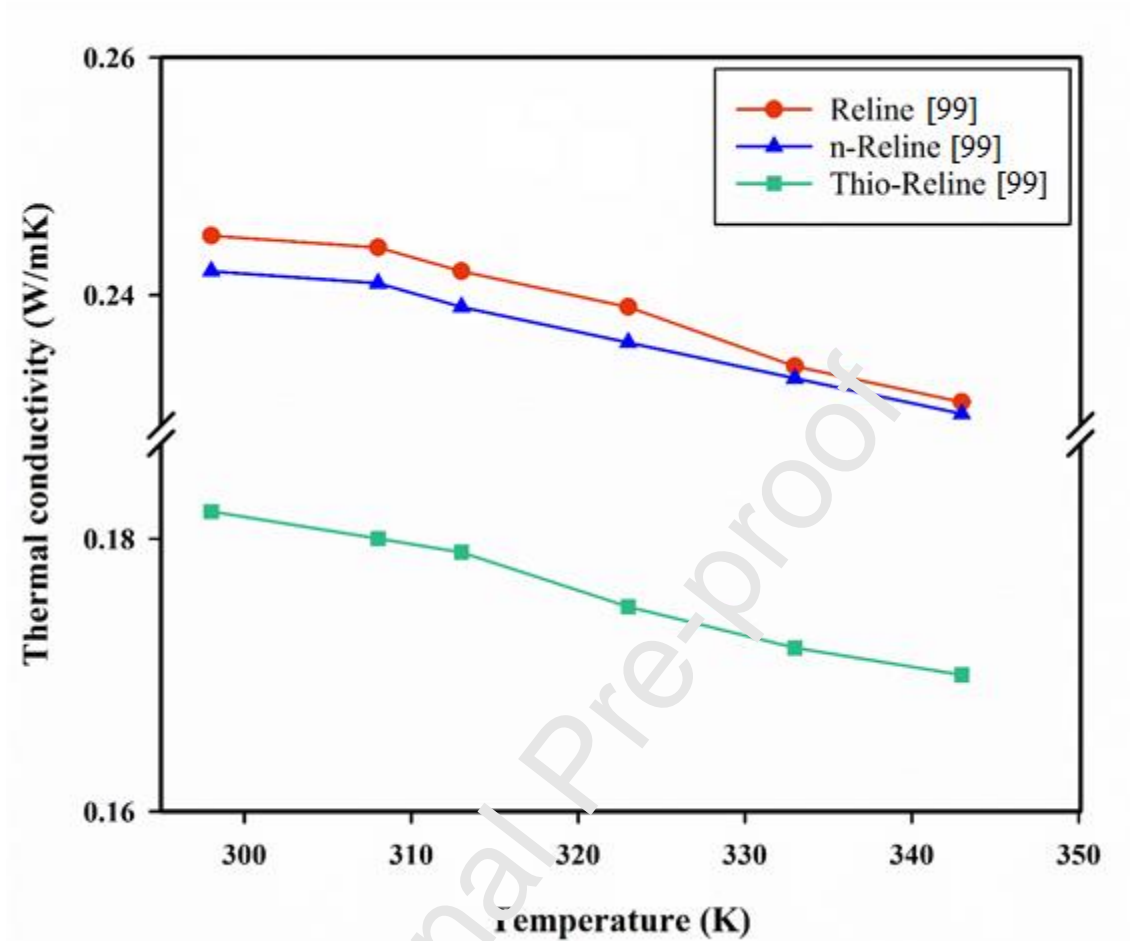


**Fig. 3.** The alteration in thermal conductivity of three different DES with temperature.

Reline: ChCl + Urea (1:1), n Reline: N,N-diethyl ethanol ammonium chloride (NDAC) + Urea (1:2), and Thio-Reline: ChCl + Thiourea (1:2).

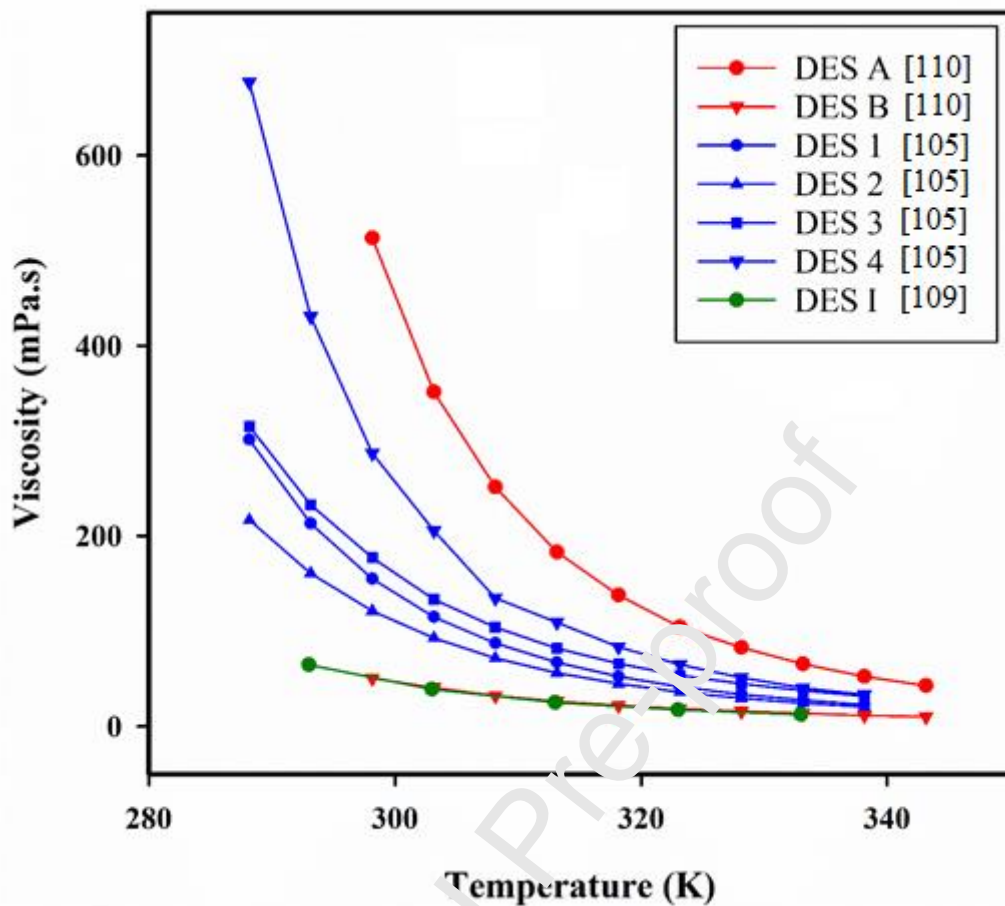


**Fig. 4.** Literature viscosity values of DESs versus the temperature.

DES A: N,N-dieyl ethanol ammonium chloride (NDAC) + Glycerol (1:2), DES B: NDAC + EG (1:2), DES 1: Tetra-butyl ammonium chloride (TBAC) + Propionic acid (PA) (1:2), DES 2: TBAC + EG (1:2), DES 3: TBAC + Polyethylene glycol (PEG) (1:2), DES4: TBAC + Phenylacetic acid (PAA) (1:2), DES I: NaBr + EG (0.5:10).

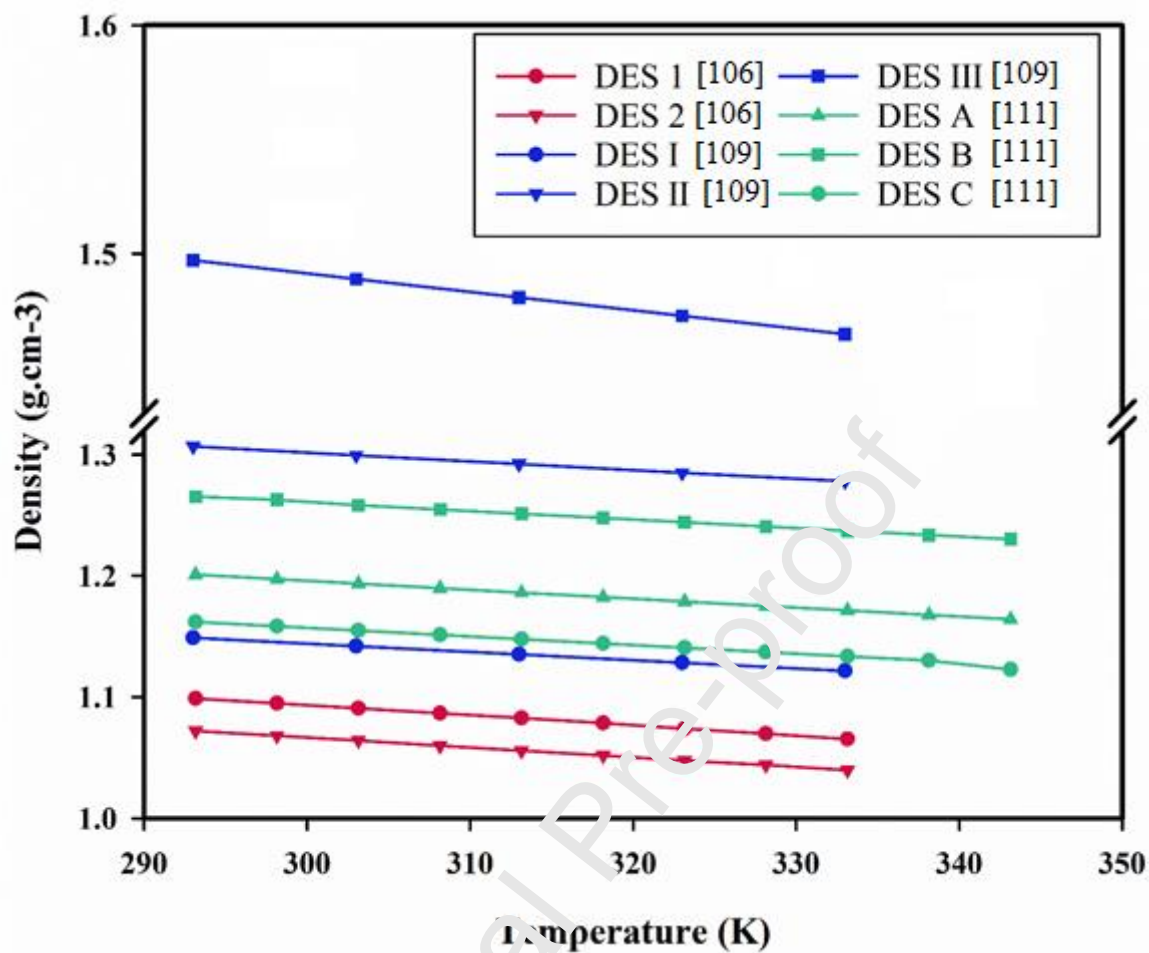


**Fig. 5.** Effect of temperature on the density of DESs.

DES 1:  $\text{ChCl} + \text{Phenol}$  (1:2), DES 2:  $\text{ChCl} + \text{p-Cresol}$  (1:2), DES I:  $\text{NaCl} + \text{EG}$  (0.5:20), DES II:  $\text{NaBr} + \text{EG}$  (0.5:10), DES III:  $\text{NaI} + \text{EG}$  (0.5:10), DES A:  $\text{L-proline} + \text{levulinic acid}$  (1:2), DES B:  $\text{L-proline} + \text{DL-lactic acid}$  (1:1), DES C:  $\text{Betaine} + \text{levulinic acid}$  (1:2).

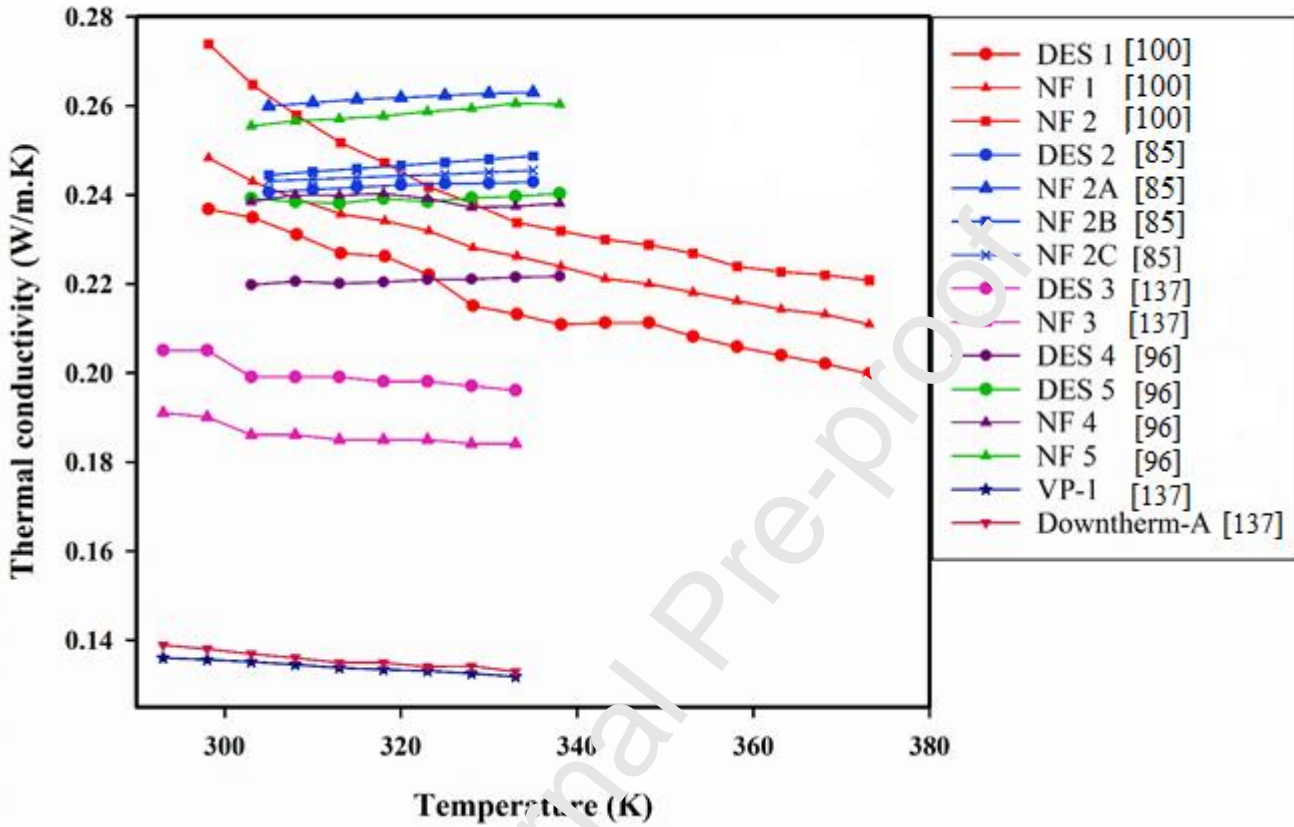


**Fig 6.** Summary of thermal conductivity versus temperature in case studies of DES as base fluid.

DES 1: DL-Menthol + Oleic acid, NF 1:  $\phi=0.001$  of  $\text{Al}_2\text{O}_3$  in DES1, NF 2:  $\phi=0.01$  in DES1, DES 2: ChCl + Glycerol, NF 2A:  $\phi=0.8\%$  of GO in DES2, NF 2B:  $\phi=0.8\%$  of  $\text{TiO}_2$  in DES2, NF 2C:  $\phi=0.8\%$  of  $\text{Al}_2\text{O}_3$  in DES2, DES 3: MTPB + EG, NF 3:  $\phi=1\%$  of  $\text{Al}_2\text{O}_3$  in DES3, DES 4: ChCl + EG, NF 4:  $\phi=4.0\%$  of  $\text{SiO}_2\text{-SH-DP-Cu}$  in DES4, DES 5: ChCl + Glycerol, NF 5:  $\phi=4.0\%$  of  $\text{SiO}_2\text{-SH-DP-Cu}$  in DES5.

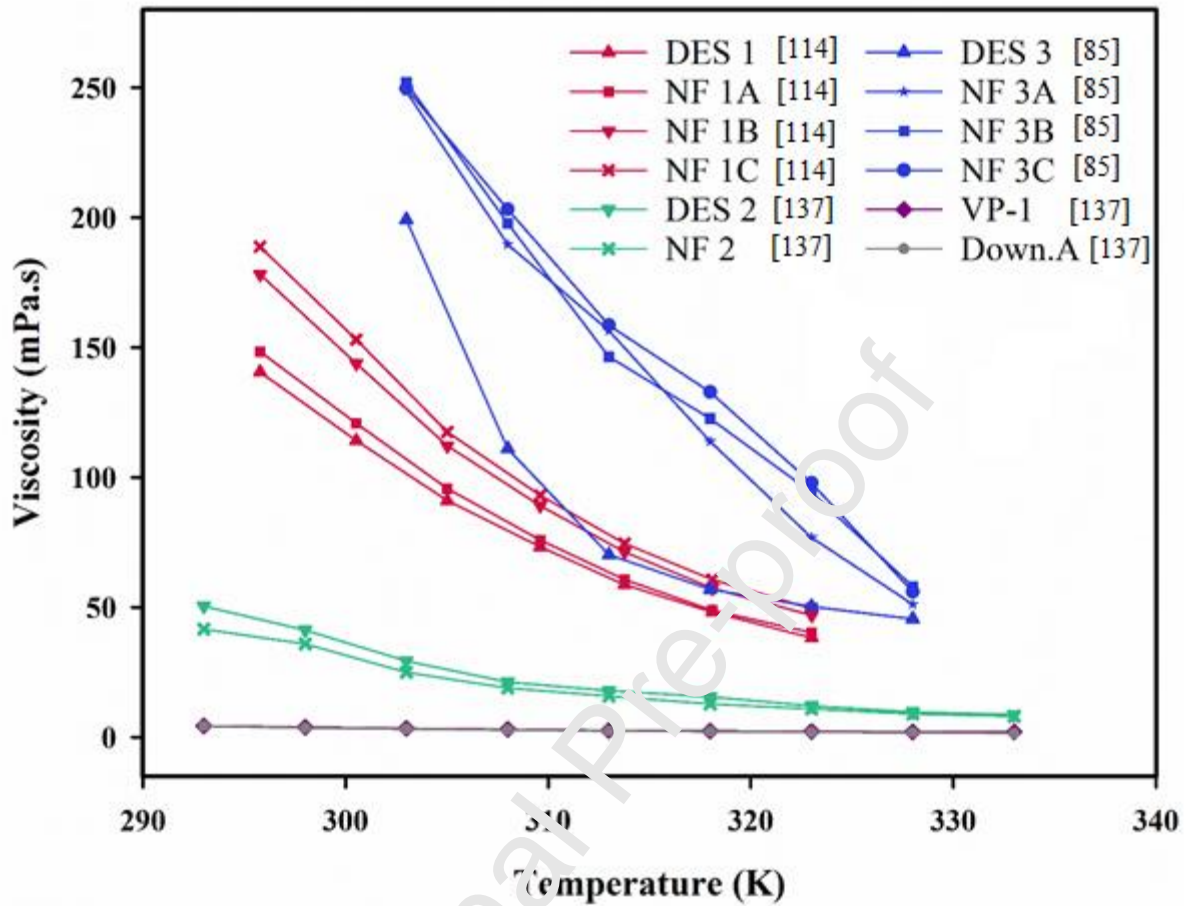


**Fig 7.** Summary of viscosity-temperature dependence in experimental studies of DES as base fluid.

DES 1: Methyl-triphenyl phosphonium bromide + EG (in 1:3 molar ratio), NF 1A:  $\phi=0.01$  of CNT in DES1, NF 1B:  $\phi=0.04$  of CNT in DES1, NF 1C:  $\phi=0.08$  of CNT in DES1, DES 2: Triphenyl phosphonium bromide + EG, NF 2: 1 wt% of  $\text{Al}_2\text{O}_3$  in DES2, DES 3: ChCl + Glycerol, NF 3A:  $\phi=1.6\%$  of GO in DES3, NF 3B:  $\phi=1.6\%$  of  $\text{TiO}_2$  in DES3, NF 3C:  $\phi=1.6\%$  of  $\text{Al}_2\text{O}_3$  in DES3.

**Kimia Jafari:** Investigation, Visualization, Data curation, Formal analysis, Writing - original draft.

**Mohammad Hossein Fatemi:** Investigation, Visualization, Data curation, Writing - review & editing.

**Patrice Estellé:** Conceptualization, Methodology, Supervision, Writing - review & editing.

Journal Pre-proof

**Declaration of interests**

The authors declare that they have no known competing financial interests or personal relationships that could have appeared to influence the work reported in this paper.

The authors declare the following financial interests/personal relationships which may be considered as potential competing interests:

Journal Pre-proof

- Thermal applicability potential of DESs and their use to produce nanofluids
- Chemical structure and preparation method of DES and DES based nanofluids
- Research findings on the DES usage as host fluid to produce nanofluids
- DESs as heat transfer fluids: overview, use, development and prospective

Journal Pre-proof